Calculating anisotropic piezoelectric properties from texture data using the MTEX open source package

David Mainprice[1*], Florian Bachmann [2],Ralf Hielscher [3], Helmut Schaeben[2], Geoffrey E. Lloyd [4]

December 15, 2013

[1]*Geosciences Montpellier UMR CNRS 5243, Université Montpellier 2, 34095 Montpellier Cedex 05, France*

[2]*Mathematische Geologie und Geoinformatik, Institut für Geophysik und Geoinformatik, Technische Universität Freiberg, 09596 Freiberg, Germany*

[3]*Fakultät für Mathematik, Technische Universität Chemnitz, 09126 Chemnitz, Germany*

[4]*School of Earth and Environment, The University, Leeds LS2 9JT, UK*

*Corresponding author (e-mail: David.Mainprice@gm.univ-montp2.fr)

Abstract

This paper presents the background for the calculation of anisotropic piezoelectric properties of single crystals and the graphical display of the results in 2 or 3 dimensions, and the calculation of the aggregate properties from constituent crystals and the texture of the aggregate in a coherent manner. The texture data can be used from a wide range of sources, from pole figure diffraction and single orientation measurements (Electron Backscattered Diffraction, Electron Channelling Pattern, Laue Pattern, Optical microscope universal-stage). We consider the elastic wave propagation in piezoelectric crystals as an example of the interaction of electrical(2^{nd} rank tensor), piezoelectric (3^{rd} rank tensor) and elastic properties (4^{th} rank tensor). In particular, we give explicit formulas for the calculation of the Voigt averaged tensor from individual orientations or from an orientation distribution function. For the latter we consider numerical integration and an approach based on the expansion into spherical harmonics. We illustrate the methods using single crystals, polycrystalline quartz measured using electron channelling patterns and ideal Curie limiting groups applied to quartz aggregates. This paper also serves as a reference paper for the mathematical tensor capabilities of the texture analysis software MTEX.

Keywords: piezoelectricity, tensors, texture, orientation density function, crystallographic preferred orientation, averaging methods, EBSD

1 Introduction

The word piezoelectricity is derived from the Greek word for to press *piezein*, hence pressure causing electricity or piezoelectricity. Piezoelectric properties are of a wide interest in sciences as the effect has now been reported in inorganic single crystals (e.g. α-quartz; Bechmann, 1958), organic crystals (e.g. sodium oxalate; Haussühl, 1991), molecular crystals (e.g. 2-furyl methacrylic anhydride; Kerkoc et al., 2009), inorganic polycrystals (e.g. ceramics; Messing et al., 2004), polymers (e.g. Hayakawa and Wada, 1973), bone (e.g. Fukada and Yasuda,1957), collagen (e.g. Fukada and Yasuda, 1964), and wood (e.g. Bazhenov, 1961). Industrial interest in piezoelectricity for transducers and resonators stems from the nature of the effect, which is either the direct effect when stress is applied to the material and a polarized electric field develops, or the converse effect is when an electric field is applied to the material it becomes strained. On April 8^{th}, 1880, Jacques Curie reported to the French Society of Mineralogy about his discovery, with the collaboration of his brother Pierre, of the direct piezoelectric effect in five crystal species examined, tourmaline (point group shown in **bold**, $\boldsymbol{3m}$), sphalerite (ZnS, $\boldsymbol{\bar{4}3m}$), boracite ($Mg_3B_7O_{13}Cl$, $\boldsymbol{mm2}$), zincite (ZnO, $\boldsymbol{6mm}$) and α-quartz (SiO_2, $\mathbf{32}$) (Curie and Curie, 1880), here we have used modern mineral names. The existence of the converse effect was predicted from thermodynamic arguments by Lippmann (1881). However, by the end of 1881 the Curie brothers had experimentally observed the converse effect and confirmed that both effects are due to the same physical property (Curie and Curie, 1882). In 1893 Jacques Curie became head lecturer in mineralogy at the University of Montpellier, where his last work was to determine the piezoelectric constants of α-quartz in 1910 before retiring due to poor health (Cady,1964). The formal description of piezoelectricity in tensor notation for all crystallographic classes is due Woldemar Voigt's major contribution summarised in his two books *Die fundamentalen physiklischen Eigenschaften der Kristalle* (1898) and the better known *Lehrbuch der Kristallphysik* (1910).

Industrial application of piezoelectric single crystals was probably first envisaged by Paul Langevin who invented an ultrasonic generator using quartz and steel plates, a precursor of modern sonar device around 1917. Subsequently the use of piezoelectric single crystals, mainly quartz, in resonators, filters and transducers became widespread. Single crystal quartz is still widely used today, along with crystals of new compositions, such as langasite, with improved characteristics (Jung and Auh,1999). Piezoelectric polycrystalline ceramics (Jaffe et al., 1971), often composed of two ferroelectric phases, are now more widely used than single crystals in transducers. Enhancing of the *crystal preferred orientations* (CPOs, or textures as they are called in Materials Science, these terms are used interchangeably in this paper as no possible confusion can result in present context) of ceramics is motivated by the need to increase the piezoelectric strain for a given applied voltage in transducer applications. Many single crystals exhibit strongly anisotropic piezoelectric properties and many aggregates of piezoelectric crystals also have strong CPOs. In polycrystalline aggregates the CPO may be due to the plastic deformation in geological samples or specially devised mechanical processing in industrial applications. In industrial processing the application of strong electric fields can be used to enhance the degree of

alignment of ferro-electric dipoles in ferroelectric crystals (*e.g.* perovskite structured double oxides $BaTiO_3$,$KNbO_3$,$KTaO_3$,$PbTiO_3$ and double fluorides $KMgF_3$,$KZnF_3$), a technique known as poling (Messing et al., 2004). CPO is often partially described by pole figures in ceramics, where as the CPO can be described completely and concisely in a quantitative manner by the *orientation density function* ODF. The combination of strong CPOs and anisotropic single crystal properties results in a strong directional variation in specimen properties, which are often difficult and time consuming to completely characterise by laboratory measurements in many directions. The evaluation of several physical properties of interest in piezoelectric materials, such as the the 2^{nd} rank dielectric permittivity, 3^{rd} rank piezoelectric strain, and 4^{th} rank elastic stiffness tensors needed for elastic wave propagation, from CPO allows the determination of aggregate properties over the complete orientation sphere of the specimen reference frame.

The estimation of physical properties of crystalline aggregates from the properties of the component crystals has been subject of extensive literature since the classical work of Voigt (1887) and Reuss (1929). Such a simple volume averaging approach is only feasible if the bulk properties of the crystals dominate the physical property of the aggregate and the effects of grain boundary interfaces can be ignored, such as the electrical conductivity along grain boundaries. In the case of piezoelectic properties the Reuss bound cannot be implemented as the piezoelectric 3^{rd} rank tensors are only transposable and not invertible, unlike 2^{nd} and 4^{th} rank centro-symmetric tensors, which are both transposable (*e.g.* 2^{nd} rank tensor T to T^{T}) and invertible (*e.g.* T to T^{-1}). A further complication in piezoelectric materials is the coupled interaction between several thermal, electrical and mechanical variables, which requires a more rigorous thermodynamic definition of the measurement of the tensor property and constitutive equations for their application to given problem as illustrated later. In this paper we will be restricted to simple Voigt volume averaging approach for aggregates and to the propagation of elastic waves in a piezoelectric material as an example of electromechanical coupling. Other averaging methods, such as self-consistent and variational effective medium methods are beyond the scope of the present paper.

A piezoelectric effect has been established either quantitatively or qualitatively in only 30% of 239 minerals that do not have a center of symmetry and should be piezoelectric (Parkhomenko, 1971). The semi-conducting elements tellurium (Te) and selenium (Se), along with mineral pyrolusite (MnO_2) have the greatest piezoelectric effect of naturally occurring compounds. Minerals with strong effect include greenockite (CdS), cadmosetite (β-CdSe) and zincite (ZnO), which have an effect 3 to 5 times greater than α-quartz. However, there are over 70 minerals that have piezoelectric effect of similar magnitude to α-quartz. Piezoelectric minerals occur most frequently in ore deposits (52 references), followed by veins and hydrothermal associations (24 references) and volcanic rocks (18 references) have been documented by Parkhomenko (1971). Ore deposits are often associated with hydrothermal activity in volcanic rocks, so these categories are not mutually exclusive. As can been seen in an area as critical to the Earth's non-renewable resources as ore deposits, piezoelectric minerals may have important role for exploration. The interest of electronic industry for piezoelectric minerals does not require development here. As show by Parkhomenko (1971) the accurate determination of the piezoelectric tensors of minerals

have only made for very small fraction of piezoelectric minerals.

Although piezoelectric minerals are not very common in the Earth's crust, at least one is very common and that is quartz, which is third most common mineral at about 12 % of the Earth's crust according to Taylor and McLennan (1985). The presence of significant volumes of quartz will influence the seismic properties of common crustal rock-types like sandstone, quartzite and granite. Some piezoelectric minerals are locally highly concentrated like sulphide and oxide minerals in ore deposits, which are the subject of intensive geophysical exploration in Russia and more recently in western countries (Bishop and Emerson,1999 ; Neishtadt et al.,2006). To our knowledge the implications of the piezoelectric effect for wave propagation of minerals has never been evaluated.

This paper is designed as a reference paper for earth and material scientists who want to use the texture analysis software `MTEX` to compute piezoelectric tensor properties of single crystals and aggregates from constituent crystal properties and the texture of the aggregate. `MTEX` is a comprehensive, freely available MATLAB toolbox that covers a wide range of problems in quantitative texture analysis, e.g. ODF modeling, pole figure to ODF inversion, EBSD data analysis, and grain modelling. The `MTEX` toolbox can be downloaded from `http://mtex.googlecode.com`. Unlike many other texture analysis programs, it offers a programming interface, which allows for the efficient processing of complex research problems in the form of scripts (M-files). The MATLAB® environment provides a wide variety of high quality graphics file format to aid publication and display of the results. In addition the `MTEX` toolbox will work identically on Microsoft Windows, Apple Mac OSX and Linux platforms in 32 and 64 bit modes with a simple installation procedure.

In `MTEX` texture analysis information like ODFs, EBSD data, pole figures, are represented by variables of different types. For example, in order to define a unimodal ODF with half-width 10°, modal preferred orientation $(10°, 20°, 30°)$ Euler angles and trigonal crystal symmetry of $\bar{3}m$, one issues the command

```
myODF = unimodalODF(orientation('Euler',10*degree,20*degree,30*degree),...
                    symmetry('-3m'),'halfwidth',10*degree)
```

which generates a variable `myodf` of type `ODF` which is displayed as

```
myODF = ODF (show methods, plot)
  crystal symmetry: -3m, X||a*, Y||b, Z||c*
  sample symmetry : triclinic

  Radially symmetric portion:
    kernel: de la Vallee Poussin, hw = 10
    center: (10,20,30)
    weight: 1
```

We will keep this style of displaying input and output to make the syntax of `MTEX` as clear as possible. Note that there is also an exhaustive interactive documentation included in `MTEX`, which explains the syntax of each command in detail. This paper is sequel to our previous paper (Mainprice et al., 2011) on the 2^{nd} and 4^{th} rank symmetric tensors of crystal and poly-crystal anisotropic physical properties. To conform with the symbols used in our previous paper we will use the symbols ε for strain, σ for stress and S for

entropy, where as in many texts on piezoelelectricty (e.g. Mason,1966; Ikeda,1990; Royer and Dieulesaint,1996; Tichý et al.,2010) the symbols S for strain, T for stress and σ for entropy are used. To avoid any potential confusion all the symbols and S.I. units used in this paper for tensors are given in Table 1.

2 Fundamentals of Piezoelectric tensors

In what follows we give the necessary background to undertake piezoelectric property calculations for single crystals, without necessarily the full mathematical developments that can be found elsewhere (e.g. Cady,1946; Mason, 1966; Nye,1985; Ikeda,1990; Newnham,2005; Tichý et al.,2010). We will restrict ourselves to linear physical properties, that are properties that can be described by a linear relationship between cause and effect, such as stress and electric field for linear piezoelectricity. Piezoelectricity is a reversible effect, so removing the stress will remove the induced electric field.

2.1 Direct and Converse effect

The first effect discovered by the Curie brothers was the direct effect. When a mechanical stress is applied to a crystal an electric polarization results. To introduce the effect we will use a simplified situation of constant entropy (adiabatic case) and temperature conditions, other variables not explicitly mentioned are also assumed constant.

The direct effect can be written as the relationship between the 2^{nd} rank stress tensor σ_{jk} and 1^{st} rank electric polarization vector P_i, linked by the piezoelectric tensor d_{ijk} as follows

$$
\begin{aligned}
P_1 &= d_{111}\sigma_{11} + d_{112}\sigma_{12} + d_{113}\sigma_{13} + d_{121}\sigma_{21} + d_{122}\sigma_{22} + d_{123}\sigma_{23} + d_{131}\sigma_{31} + d_{132}\sigma_{32} + d_{133}\sigma_{33},\\
P_2 &= d_{211}\sigma_{11} + d_{212}\sigma_{12} + d_{213}\sigma_{13} + d_{221}\sigma_{21} + d_{222}\sigma_{22} + d_{223}\sigma_{23} + d_{231}\sigma_{31} + d_{232}\sigma_{32} + d_{233}\sigma_{33},\\
P_3 &= d_{311}\sigma_{11} + d_{312}\sigma_{12} + d_{313}\sigma_{13} + d_{321}\sigma_{21} + d_{322}\sigma_{22} + d_{323}\sigma_{23} + d_{331}\sigma_{31} + d_{332}\sigma_{32} + d_{333}\sigma_{33}.
\end{aligned}
$$

The electric polarization is the electric dipole moment per unit volume, which is proportional to the electric field defined by $P_i = \kappa_0 \chi_{ij} E_j$ where κ_0 is the permittivity of a vacuum $8.854188x10^{-12}$ C/Vm, χ_{ij} is the dielectric susceptibility tensor in F/m, and E_j the electric field strength in V/m. We will use the more compact tensor notation with the summations presented explicitly

$$P_i = \sum_{j=1}^{3}\sum_{k=1}^{3} d_{ijk}\sigma_{jk}, \;\; i = 1, 2, 3,$$

or using the implicit Einstein summation convention; when an index occurs twice in the same term, summation with respect to that index is to be understood. For example, it is understood that summations occur for indices j and k for direct effect as they occur twice in d_{ijk} and σ_{jk} on the right-hand side of the equation

$$P_i = d_{ijk}\sigma_{jk},$$

where P_i is electric polarization, d_{ijk} the piezoelectric tensor and σ_{jk} the stress tensor. The converse effect can be written as

$$\varepsilon_{jk} = \sum_{i=1}^{3} d_{ijk} E_i (j,k = 1,2,3) \text{ or } \varepsilon_{jk} = d_{ijk} E_i,$$

where ε_{ij} is the elastic strain tensor and E_k is the electric field vector. Here again the summation is understood for the index i occurring in d_{ijk} and E_i. As 1^{st} rank electric polarization P_i and electric field E_k vectors have the index $i = 1, 2$ or 3 and 2^{nd} rank stress σ_{jk} and elastic strain ε_{jk} tensors have indices $j = 1, 2$ or 3 and $k = 1, 2$ or 3, hence the 3^{rd} rank piezoelectric tensor d_{ijk} has $3 \times 3 \times 3 = 27$ coefficients. The symmetric nature of the stress and strain 2^{nd} rank tensors for linear elasticity results in interchangeability of jk and kj indices of piezoelectric tensor d_{ijk}, which reduces the number of independent components from 27 to 18 where $d_{ijk} = d_{ikj}$, but $d_{ijk} \neq d_{jik}$.

In the literature the tensor d_{ijk} is reported for single crystals in the practical and compact Voigt matrix notation. The conversion from Voigt notation d_{in} to tensor d_{ijk} notation $d_{ijk} = d_{in}$ when $n = 1, 2, 3$ and $d_{ijk} = \frac{1}{2} d_{in}$ when $n = 4, 5, 6$. The factor of $\frac{1}{2}$ is due to the difference between the strain tensor and "engineering" shear strains of Voigt matrix notation. The piezoelectric tensor will always have three indices and Voigt matrix notation two indices. The direct and converse effects can also be written in Voigt matrix notation as

$$P_i = \sum_{n=1}^{6} d_{in} \sigma_j, \;\; i = 1,2,3, \;\; \text{and} \;\; \varepsilon_j = \sum_{i=1}^{3} d_{ni} E_i, \;\; n = 1,2,3,4,5,6.$$

Alternatively we can write the direct and converse effects in reduced matrix notation **bold** type (see Bond, 1943; Bishop, 1981; Russell and Ghomshei, 1997 for tensor examples using the matrix method) or full Voigt matrix and vector notation

$$\boldsymbol{P} = \boldsymbol{d}\,\boldsymbol{\sigma} = \begin{pmatrix} P_1 \\ P_2 \\ P_3 \end{pmatrix} = \begin{pmatrix} d_{11} & d_{12} & d_{13} & d_{14} & d_{15} & d_{16} \\ d_{21} & d_{22} & d_{23} & d_{24} & d_{25} & d_{26} \\ d_{31} & d_{32} & d_{33} & d_{34} & d_{35} & d_{36} \end{pmatrix} \begin{pmatrix} \sigma_1 \\ \sigma_2 \\ \sigma_3 \\ \sigma_4 \\ \sigma_5 \\ \sigma_6 \end{pmatrix}$$

$$\boldsymbol{\varepsilon} = \boldsymbol{d}^{\mathsf{T}} \boldsymbol{E} = \begin{pmatrix} \varepsilon_1 \\ \varepsilon_2 \\ \varepsilon_3 \\ \varepsilon_4 \\ \varepsilon_5 \\ \varepsilon_6 \end{pmatrix} = \begin{pmatrix} d_{11} & d_{21} & d_{31} \\ d_{12} & d_{22} & d_{32} \\ d_{13} & d_{32} & d_{33} \\ d_{14} & d_{24} & d_{34} \\ d_{15} & d_{25} & d_{35} \\ d_{16} & d_{26} & d_{36} \end{pmatrix} \begin{pmatrix} E_1 \\ E_2 \\ E_3 \end{pmatrix}$$

If we now write the matrix $\boldsymbol{d}$ in partial differential form and a table format so it is easy to understand that the direct and converse effects requires that the tensor $\boldsymbol{d}$ is in units of

Coulomb/Newton and its transpose $\boldsymbol{d}^{\mathsf{T}}$ in units of metre/Volt, this will also apply to the other piezoelectric tensors that we will introduce later.

$$\boldsymbol{d} = d_{in} \equiv \frac{\partial \sigma_n}{\partial P_i} \equiv$$

	σ_1	σ_2	σ_3	σ_4	σ_5	σ_6
P_1	d_{11}	d_{12}	d_{13}	d_{14}	d_{15}	d_{16}
P_2	d_{21}	d_{22}	d_{23}	d_{24}	d_{25}	d_{26}
P_3	d_{31}	d_{32}	d_{33}	d_{34}	d_{35}	d_{36}

$$\boldsymbol{d}^{\mathsf{T}} = d_{ni} \equiv \frac{\partial E_i}{\partial \varepsilon_n} \equiv$$

	E_1	E_2	E_3
ε_1	d_{11}	d_{21}	d_{31}
ε_2	d_{12}	d_{22}	d_{32}
ε_3	d_{13}	d_{23}	d_{33}
ε_4	d_{14}	d_{24}	d_{34}
ε_5	d_{15}	d_{25}	d_{35}
ε_6	d_{16}	d_{26}	d_{36}

2.2 Symmetry and rotation

All crystals belong which centrosymmetric points groups (*i.e.* the 11 Laue classes) are piezoelectrically inactive. All crystals belong the 21 non-centrosymmetric points groups are piezoelectrically active, with the exception of the cubic **432**. In the **432** point group due to the presence of four-fold axes parallel to [100], [010] and [001], which make all directions perpendicular to these axes non-polar (Hermann, 1934) and results in all tensor coefficients that are non-zero ($d_{14} = d_{25} = d_{36}$) in the two other piezoelectric cubic points groups (**23** and $\bar{\mathbf{4}}$**3m**) being zero in **432**. Hence there are 20 non-centrosymmetric points groups for piezoelectric active crystals, of which 10 enantiomorphic space group pairs that do not have improper rotations (*i.e.* no mirror planes), and hence crystals occur in right-handed and left-handed forms(*e.g.* α-quartz) are distributed in 6 point groups (**4**, **422**, **3**, **32**, **6**, and **622**). Standard texture orientation determination using diffraction based measurements that obey Friedel's law can be routinely made for non-enantiomorphic piezoelectric crystals where the diffraction intensity of planes (**hkl**) and ($\bar{\mathbf{h}}\bar{\mathbf{k}}\bar{\mathbf{l}}$) are the same because of the centre of symmetry that is imposed by the diffraction process. To distinguish the right-handed and left-handed forms of enantiomorphic crystals will require additional information, such as dynamical scattering revealing a violation of Friedel's law (e.g. Bunge and Esling, 1985; Goodman and Johnston, 1977; Goodman and Secomb, 1977; Marthinsen and Hϕier, 1988). Alternatively gyration, also called optical activity, can be used in optically transparent crystals(e.g. Wenk, 1985) to detect the handedness of crystal.

Piezoelectric tensors, like all 3^{rd} rank tensors, obey the transformation laws such that $P'_{ijk} = a_{il}a_{jm}a_{kn}P_{lmn}$, where a_{il} *etc* are rotation matrices ($a^{\mathsf{T}} = a^{-1}$) which changes the orientation of the piezoelectric tensor P_{lmn} to some new orientation in specimen coordinates P'_{ijk}. The application of a rotation that belongs to the point group of crystal symmetry the tensor will be invariant. Typically an orientation in `MTEX` can be defined by Euler angles, quaternions and axis/angle pairs.

For a crystal with point group symmetry **1** there are no intrinsic symmetry rotations or mirror planes that will reduce the number of non-zero coefficients from the 18 of the (3×6) Voigt matrix format of the piezoelectric tensor for a triclinic crystal. If the crystal has higher symmetry, like the monoclinic point group **2** with a two-fold 180° rotation about either the **b**-axis or the **c**-axis depending on the crystallographic setting, this has only 8 independent non-zero coefficients. With the increasing number of symmetry operations the number of non-zero coefficients reduces to one for hexagonal $\bar{\mathbf{6}}\mathbf{2m}$ and cubic $\bar{\mathbf{4}}\mathbf{3m}$ and **23** point groups.

2.3 The crystal reference frame

Matter tensors describing physical properties like piezoelectricity of a single crystal or poly-crystalline specimen require tensor a reference frame. In the case of single crystals the reference frame must be defined with respect to the crystal structure in terms of crystallographic directions, where as for poly-crystalline specimen it must be defined in specimen coordinates. We will restrict ourselves to tensors of single or polycrystals defined in a Cartesian reference frame comprising 3 unit vectors, $\boldsymbol{X}$, $\boldsymbol{Y}$, $\boldsymbol{Z}$. The use of an orthogonal reference frame for single crystals avoids the complications of the metric associated with the crystal unit cell. In any case, almost all modern measurements of physical property tensors are reported using right-handed Cartesian reference frames.

We have previously discussed how the single crystal tensor reference frame is defined using the crystal coordinate system in Mainprice et al.(2011). Here we will illustrate the definition of the crystal symmetry frame in `MTEX` using the example of right-handed single crystal of α-quartz.

In `MTEX` the alignment of the crystal reference frame is defined together with the symmetry group and the crystal coordinate system. For the case of 3^{rd} rank tensor like piezoelectricity we need to define the point group symmetry rather than the Laue class that is sufficient for symmetric 2^{nd} and 4^{th} rank tensors as illustrated in `MTEX` by Mainprice et al.(2011). For example α-quartz is in Laue class $\bar{\mathbf{3}}\mathbf{m}$ which imposes a center of symmetry it does not have physically, the point group **32** has no centre of symmetry and is compatible with piezoelectric properties of α-quartz. The information is stored in a variable of type `symmetry`. For example for α-quartz the point group symmetry is **32**, the axes lengths are $a = b = 4.9134\mathring{A}$ and $c = 5.4052\mathring{A}$, $\alpha = \beta = 90°$ and $\gamma = 120°$. As `MTEX` recognizes that point group symmetry is **32** has trigonal symmetry there is no need to enter the cell angles in `symmetry`. Next comes the definition of the the Cartesian tensor reference X, Y, Z frame, X is parallel to the a-axis and Z is parallel to c-axis.

```
cs_tensor = symmetry('32',4.9134  4.9134  5.4052], 'X||a', 'Z||c',...
  'mineral', 'RH alpha-Quartz');
```

```
cs_tensor = symmetry (size: 1)

  mineral           : RH alpha-Quartz
  symmetry          : 32 (-3m)
  a, b, c           : 4.9, 4.9, 5.4
```

```
  alpha, beta, gamma: 90, 90, 120
  reference frame   : X||a, Y||b*, Z||c
```

When defining a crystal piezoelectric tensor $\boldsymbol{d}$ with respect to this crystal reference frame the variable `cs_tensor` becomes part of the newly generated tensor object $\boldsymbol{d}$ and in this way the tensor coefficients and the tensor reference frame are stored together, for example,

```
% Enter Piezoelectric (strain) tensor (d_ij) as (3 by 6) matrix
% Md line by line in pC/N
% Ogi, H., Ohmori, T. Nakamura, N. and Hirao M. (2006)
% RH alpha-quartz d11 = -1.9222  d14 = -0.1423
Md =[[-1.9222   +1.9222     0      -0.1423     0          0     ];...
     [   0        0         0        0       +0.1423    3.8444];...
     [   0        0         0        0         0          0     ]];
d = tensor(Md, cs_Tensor, 'rank',3, 'propertyname',...
    'piezoelectric_strain_tensor', 'unit', 'pC/N', 'DoubleConvention')
```

```
d = tensor (show methods, plot)
  propertyname    : piezoelectric strain tensor
  unit            : pC/N
  rank            : 3 (3 x 3 x 3)
  doubleConvention: true
  mineral         : RH alpha-Quartz (32, X||a, Y||b*, Z||c*)

  tensor in compact matrix form:
 -1.9222  1.9222       0 -0.1423       0       0
       0       0       0       0  0.1423  3.8444
       0       0       0       0       0       0
```

defines the piezoelectric tensor $\boldsymbol{d}$ in pC/N of right-handed α-Quartz. In this case we need to specify `DoubleConvention` so that `MTEX` knows that this tensor transforms Voigt to tensor notation as $d_{ijk} = d_{in}, n = 1, 2, 3$, and $d_{ijk} = \frac{1}{2} d_{in}, n = 4, 5, 6$. The transformation from Voigt to tensor notation and vice-versa will be discussed in more detail later.

2.4 Longitudinal Surfaces and other representations of tensors

The single crystal piezoelectric tensor can be visualized in several ways. The base of all visualizations is the value of the tensor $\boldsymbol{d}$ in a direction $\boldsymbol{x}$, or dvalue($\boldsymbol{x}$) which is given by

$$\text{dvalue}(\boldsymbol{x}) = x_i x_j x_k d_{ijk}.$$

To compute the dvalue($\boldsymbol{x}$) in `MTEX` we first need to define a direction relative to the tensor reference frame. This is done by the command `Miller`. The following syntax is supported

- by coordinates with respect to the Euclidean crystal reference frame X, Y, Z

```
x = Miller(1,0,0,'xyz',cs_tensor)
```

- by coordinates with respect to the crystal directions a, b, c

```
x = Miller(1,0,0,'uvw',cs_tensor)
```

- by coordinates with respect to the reciprocal coordinate system a^*, b^*, c^*

```
x = Miller(1,0,0,'hkl',cs_tensor)
```

- by polar coordinates

```
x = Miller(polar_angle,azimuth_angle,'polar',cs_tensor)
```

Note that again the variable `cs_tensor` is passed on to the definition of the direction to make clear that the coordinates are given with respect to this specific reference frame.Now we can use the command `directionMagnitude` to compute dvalue($\boldsymbol{x}$)

```
dvalue  = directionalMagnitude(d,Miller(1,0,0,'xyz',cs_tensor))
```

```
dvalue =  -1.9222
```

with vector3d $\mathbf{x}$ = vector3d(1,0,0), the result is -1.9222 pC/N as expected for a positive a-axis when $X \| a$, and for vector3d(0.5,0.8660,0) it is 1.9222 pC/N as expected for a negative a-axis. For the direction vector3d(0,0,1) parallel to the c-axis the value for $\mathbf{d}$ is zero as this is not polar direction.

```
% positive a-axis (1.0,0.0,0.0)
positive_a_axis = xvector
dvalue = directionalMagnitude(d,xvector)
dvalue =  -1.9222
% alternative use uvtw = +a1[2,-1,-1,0]
dvalue = directionalMagnitude(d,vector3d(Miller(2,-1,-1,0,cs_Tensor,'uvw')))
% negative a-axis (0.5,0.8660,0.0)
polar_angle = 90*degree
azimuth_angle = 60*degree
negative_a_axis = vector3d('polar',polar_angle,azimuth_angle)
dvalue = directionalMagnitude(d,negative_a_axis)
dvalue =  1.9222
% alternative use uvtw = -a[1,1,-2,0]
dvalue = directionalMagnitude(d,vector3d(Miller(1,1,-2,0,cs_Tensor,'uvw')))
```

Perhaps the most classical representation of piezoelectricity is the longitudinal surface. The longitudinal surface of infinitesimal area is normal to an axial tensile stress parallel to $x_1^{'}$, the polarization normal to the surface is given by $P_1^{'} = d_{111}^{'}\sigma_{11}^{'}$, and $d_{111}^{'}$ gives the polarization value parallel to $x_1^{'}$ for unit stress. The longitudinal surface is defined by the radius vector $\mathbf{r}$ parallel direction $x_1^{'}$, which was previously in the orientation x_1

$$\boldsymbol{r} = d_{111}^{'} = a_{1i}a_{1j}a_{1k}d_{ijk} \;\; or \;\; \boldsymbol{r} = d_{222}^{'} = a_{2i}a_{2j}a_{2k}d_{ijk} \;\; or \;\; \boldsymbol{r} = d_{333}^{'} = a_{3i}a_{3j}a_{3k}d_{ijk}$$

from this we can understand that radius vector $\boldsymbol{r}$ is rotated in the XYZ tensor frame to map the longitudinal surface, where $\boldsymbol{r} = d_{111}^{'} = \text{dvalue}(\boldsymbol{x})$ (Figure 1).

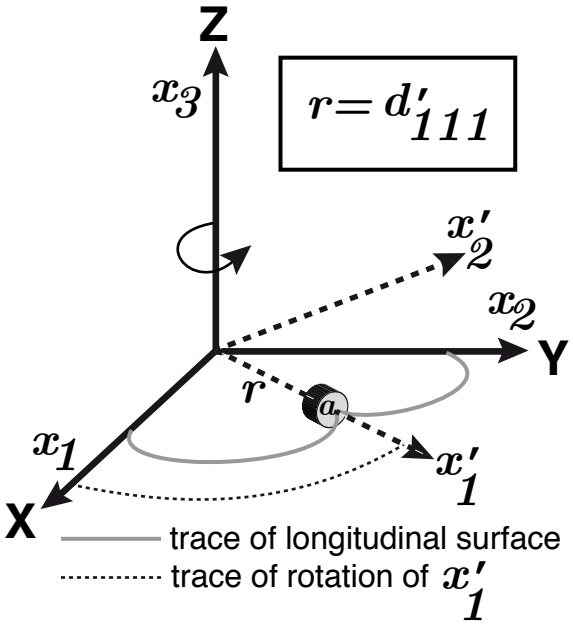

Figure 1: Schematic illustration of the construction of the longitudinal surface by the rotation of $x_1^{'}$ about the **Z** axis with $d_{111}^{'}$ = dvalue($\boldsymbol{x}$), **a** represents the infinitesimal surface area.

The surface can be plotted in a 2D section normal to any direction defined by a MTEX vector3d in the tensor coordinate frame. For example to plot the surface in the basal (0001) plane we use the predefined zvector = vector3d(0,0,1) as $Z \| c$, and plot the plane normal to the predefined yvector = vector3d(0,1,0) which is a 1^{st} order prism plane (m) containing the a- and c-axes, Figure 2. Using the MTEX plot command with the option 'section' will plot the 2D longitudinal surface, which is the limiting surface between positive and negative values of the tensor $\boldsymbol{d}$. In regions outside these longitudinal limiting surfaces no polarization is possible.

```
plot(d,'section',zvector)
% alterative use uvtw = c[0,0,0,1]
plot(d,'section',vector3d(Miller(0,0,0,1,cs_Tensor,'uvw'))
plot(d,'section',yvector)
% alterative use uvtw = m[0,1,-1,0]
plot(d,'section',vector3d(Miller(0,1,-1,0,cs_Tensor,'uvw'))
```

In MTEX the magnitude of a piezoelectric tensor can be plotted as a function of crystal direction in the tensor frame on an equal area stereogram, either as the crystallographic asymmetric unit, as a complete hemisphere or even as both hemispheres. The plot of both hemispheres shows the 3D distribution of the piezoelectric tensor $\boldsymbol{d}$ values in pC/N, where the maximum negative value (white) is parallel to the three $+a$-axes and the value parallel to the c-axis is zero Figure 3. The upper and lower hemisphere distributions are identical.

```
plot(d,'complete')
```

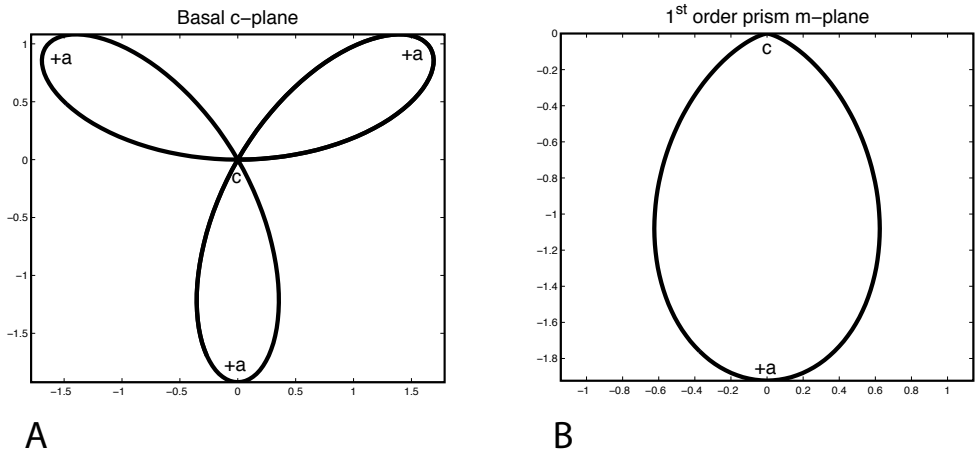

Figure 2: Right-handed α-quartz **32** : plot of longitudinal surfaces of the piezoelectric tensor $\boldsymbol{d}$ A) basal plane (c) B) 1^{st} order prism plane (m). Units pC/N

```
colorbar
annotate([xvector,yvector,zvector],'label',...
{'X||+a','Y||m','Z||c'},'backgroundcolor','w','FontSize',18);
```

To better understand the distribution of the piezoelectric tensor $\boldsymbol{d}$ a perspective 3D plot can be used, that can be rotated interactively using the command `rotate3d` in the Matlab environment. The figure 4 and 5 can be made using the command `plot`. We will illustrate for the α-quartz (Figure 4) and mineral sphalerite (ZnS) also know as zincblende (Figure 5). Sphalerite is an important mineral in zinc-bearing mining deposits (e.g. Bishop and Emerson, 1999). The symmetry of sphalerite is cubic $\bar{\mathbf{4}}\mathbf{3m}$ point group where the only non-zero independent value of tensor $\boldsymbol{d}$ is d_{14} with tensor having three non-zero coefficients d_{14}=d_{25}=d_{36}. The $\bar{\mathbf{4}}\mathbf{3m}$ point group has a set of 24 symmetry operations, it has no proper (rotational) 4-fold axis, only 4-fold inversion axes parallel to a,b and c-axes.

```
% crystal symmetry (cs)
cs_tensor = symmetry('-43m', [5.41 5.41 5.41],...
[90.0000 90.000 90.000]*degree, 'X||a', 'Z||c','mineral','Sphalerite')
%
% Enter Piezoelectric (strain) tensor (d_ij) as (3 by 6) matrix
% Md line by line in pC/N
% Berlincourt,D., Jaffe, H., and Shiozawa, L.R. (1963)
% Physical Review 129, 1009-1017.
% Sphalerite (ZnS) d14 = 3.180 pC/N
Md =[ [ .00 .00 .00 3.18 .00 .00];...
      [ .00 .00 .00 .00 3.18 .00];...
      [ .00 .00 .00 .00 .00 3.18]];
d = tensor(Md, cs_Tensor,'rank',3,'propertyname',...
    'piezoelectric_strain_tensor','unit','pC/N','DoubleConvention')
% plot
plot(d,'3d')
```

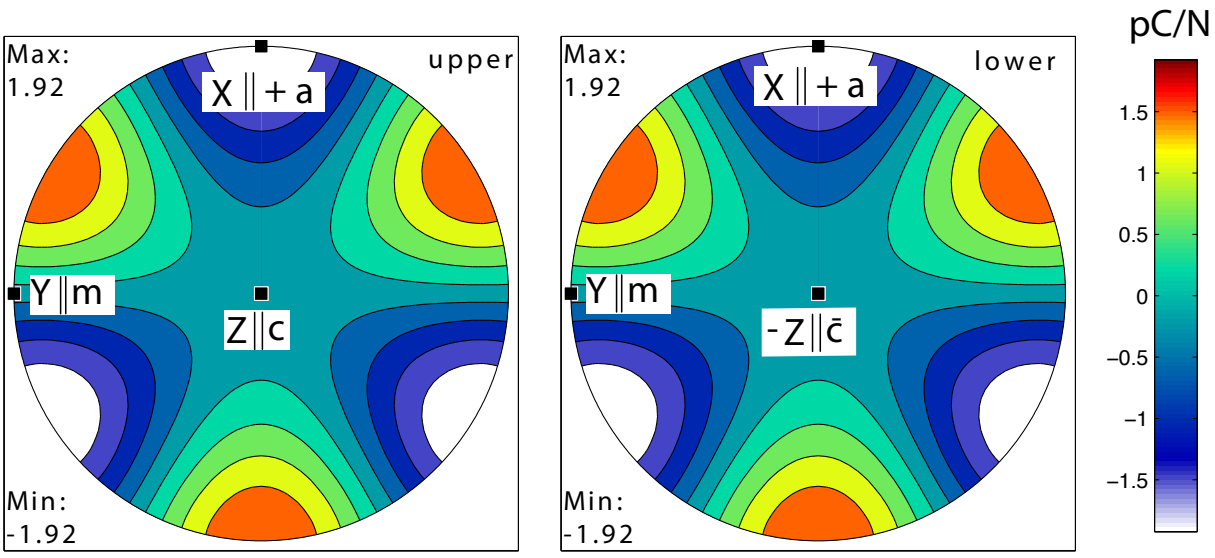

Figure 3: Right-handed α-quartz **32** : upper and lower hemisphere plots of the piezoelectric tensor $\boldsymbol{d}$ using 'complete' with default filled contour option and the `MTEX` annotate command

```
% activate MATLAB 3d interactive rotation of plot
rotate3d
```

```
cs_tensor = crystal symmetry (show methods, plot)

  mineral : Sphalerite
  symmetry: -43m (m-3m)

d = tensor (show methods, plot)
  propertyname     : piezoelectric strain tensor
  unit             : pC/N
  rank             : 3 (3 x 3 x 3)
  doubleConvention: true
  mineral          : Sphalerite (-43m)

  tensor in compact matrix form:
    0    0    0 3.18    0    0
    0    0    0    0 3.18    0
    0    0    0    0    0 3.18
```

Finally, we should point out for two crystal symmetry point groups **422** and **622** there is no longitudinal effect. In these two groups there is only one independent piezoelectric coefficient d_{14}. If we write out the full equation for the long longitudinal effect for these symmetry groups we have in tensor notation

$$d'_{111} = a_{11}a_{12}a_{13}2d_{123} + a_{12}a_{11}a_{13}2d_{213}$$

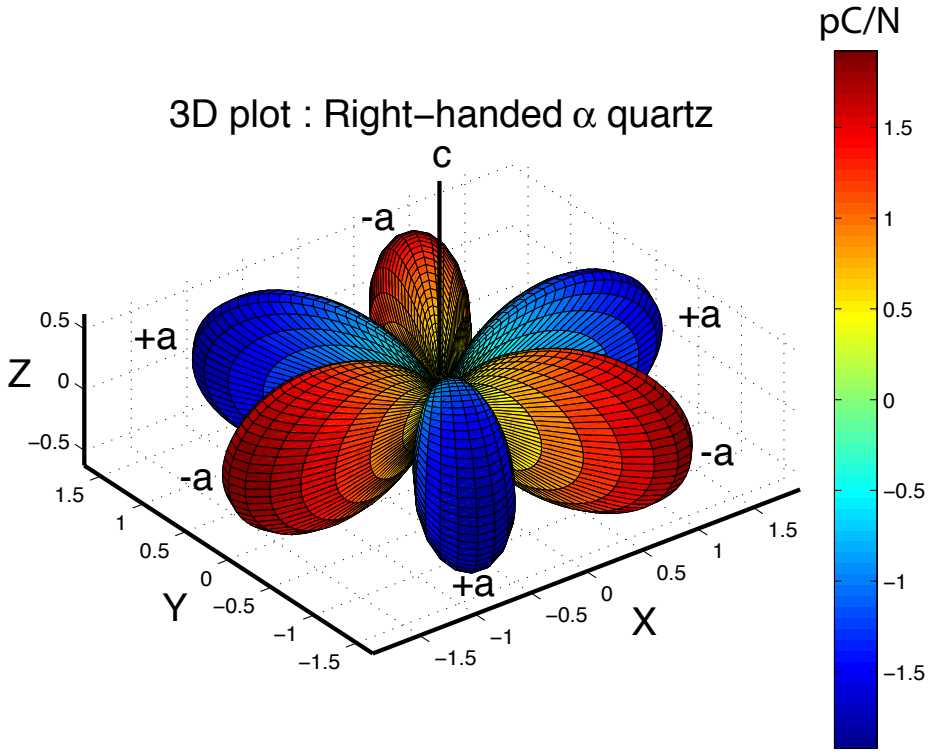

Figure 4: Right-handed α-quartz **32** : 3D plot of the piezoelectric tensor $\boldsymbol{d}$ using plot(d,'3D'). Note the 3-fold c-axis repeating the red (positive) and blue (negative) lobes, 2-fold a-axes, $+a$-axes have negative values, and the zero value along the c-axis.

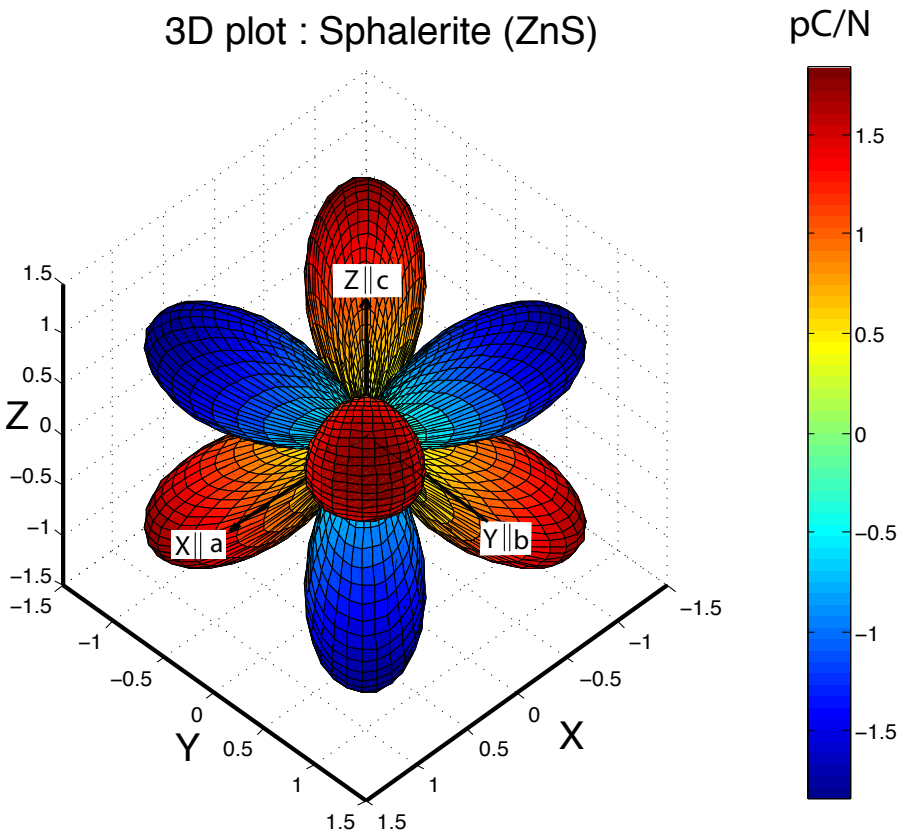

Figure 5: Sphalerite $\bar{4}\mathbf{3m}$: 3D plot of the piezoelectric tensor $\boldsymbol{d}$ using plot(d,'3D'). Note the 3-fold [111] cube axes repeating the red (positive) and blue (negative) lobes and 2-fold axes along a, b and c.

and in Voigt notation

$$d_{11}^{'} = a_{11}a_{12}a_{13}(d_{14} + d_{25})$$

In these symmetry groups $d_{14} = -d_{25}$ then $d_{11}^{'} = 0$. Hence no longitudinal effect and no polar axes are present and electric polarization can only be generated by shear. Two examples are β-quartz point group **622**, d_{14}=-1.86 pC/N (about two times that of α-quartz) at 612°C (Cook and Weissler,1950) and Paratellurite (α-TeO_2) point group **422**, d_{14}=12.41 pC/N (Ogi et al.,2004).

2.5 Hydrostatic Effect

The hydrostatic effect is simply described by the direct piezoelectic effect, where the electric field is considered to be constant and D vector of electric displacement is equal to the polarization P, so that

$$P_i = D_i = d_{ijk}\sigma_{jk}.$$

The hydrostatic pressure p is given by $\sigma_{jk} = -p\delta_{jk}$, where δ_{jk} is the Kronecker delta,

$$P_i = -d_{ikk}p.$$

The hydrostatic effect is conveniently defined by the 3 orthogonal components parallel to tensor frame X,Y,Z in Voigt matrix notation. In Voigt notation tensor components related to normal stresses are (d_{in} where i=1,2,3, n=1,2,3) and those that involve shear stresses (d_{in} where i=1,2,3, n=4,5,6). Obviously only the coefficients related normal stress are compatible with hydrostatic stress.

$$\begin{aligned} P_1 &= -(d_{11} + d_{12} + d_{13})p \\ P_2 &= -(d_{21} + d_{22} + d_{23})p \\ P_3 &= -(d_{31} + d_{32} + d_{33})p \end{aligned}$$

The hydrostatic piezoelectric coefficient (Tichý et al.,2010) is defined as scalar in the fixed single crystal X,Y and Z tensor co-ordinate frame

$$d_h = (d_{11} + d_{12} + d_{13}) + (d_{21} + d_{22} + d_{23}) + (d_{31} + d_{32} + d_{33})$$

d_h has to be a non-zero value, after taking into account the action of symmetry on the signs and magnitudes of d_{ij}. The hydrostatic effect is only present in 10 crystal points groups ($\bar{\mathbf{1}}$, **2**, **m**, **mm2**, **4**, **4mm**, **3**, **3m**, **6**, **6mm**) out of 20 for piezoelectric crystals. For 7 crystal point groups the hydrostatic polarization only occurs along the c-axis direction (Klapper and Hahn, 2006), this requires after symmetry of the tensor is taken into account that

$$d_h = 2d_{31} + d_{33}$$

for (**4**, **4mm**, **3**, **3m**, **6**, **6mm**) and

$$d_h = d_{31} + d_{32} + d_{33}$$

for (**mm2**). For point group (**2**) with 2-fold and the hydrostatic effect along the b-axis

$$d_h = d_{21} + d_{22} + d_{23}$$

For point group (**m**) with two-fold along b-axis and effect along $[u0w]$ directions

$$d_h = (d_{11} + d_{12} + d_{13}) + (d_{31} + d_{32} + d_{33})$$

For point group ($\bar{\mathbf{1}}$) all directions $[uvw]$ are possible

$$d_h = (d_{11} + d_{12} + d_{13}) + (d_{21} + d_{22} + d_{23}) + (d_{31} + d_{32} + d_{33}).$$

The only common minerals exhibiting the hydrostatic effect are the tourmaline group (**3m**), wurtzite group (**6mm**), oxides with perovskite structure and all minerals that are pyroelectric as the same symmetry constraints apply. The presence of pressure in almost all geological situations could potentially generate electrical polarization if piezoelectric minerals are present, however relatively few minerals exhibit the hydrostatic effect. Some special situations may occur in zinc-bearing mining deposits where two piezoelectric polymorphs of ZnS, sphalerite ($\bar{\mathbf{4}}$**3m**) without a hydrostatic effect and wurtzite (**6mm**) with a hydrostatic effect are often associated. It is also interesting to note that several common sulfide ore minerals bismuthinite (Bi_2S_3 **mm2**), chalcocite (Cu_2S **2/m**), pyrrhotite ($Fe_{(1-x)}$ S_x **6/mmm**), and stibnite (Sb_2S_3 **mm2**) are ferroelectric (Corry,1994), of which bismuthinite and stibnite occur in piezoelectric point groups. The piezoelectric effect has been used extensively for geophysical exploration for mining industry in Russia (Neishtadt et al.,2006). The hydrostatic effect has many industrial applications, such as pressure measurement and underwater sonar, where historically tourmaline has be used in these sonar devices. We will use the tensor coefficients recently measured for tourmaline of Pandey and Schreuer (2012) to illustrate the calculation of d_h. Tourmaline has symmetry **3m** where the only non-zero coefficients involving normal stresses are d_{21} d_{22} d_{31} d_{32} and d_{33} where by symmetry $d_{21} = -d_{22}$ so their combined effect is zero, the remaining non-zero terms are $d_h = d_{31} + d_{32} + d_{33} = 0.16 + 0.16 + 1.91 = 2.23$ pC/N.

2.6 Constitutive equations

The constitutive equations define the coupling between independent variables. To visualize the relationships between different variables of electric field $\boldsymbol{E}$, electric displacement $\boldsymbol{D}$, strain $\boldsymbol{\varepsilon}$, stress field $\boldsymbol{\sigma}$, temperature $\mathbf{T}$ and entropy $\mathbf{S}$, Heckmann (1925) introduced a triangular diagram (Figure 6A). From this triangular diagram we have chosen the 4 variables stress, strain, electric field and electric displacement associated with piezoelectricity, which is equivalent to setting the variables entropy and temperature to constant values for the constitutive equations we have chosen to present. The constitutive or coupled equations are given below are taken from Mason(1966), other equations are given by Ikeda (1990). A pair of constitutive equations is required to describe the mechanical and electrical behaviour of piezoelectric crystal. The equations are given in tensor and matrix notation

as **bold** characters. In matrix notation the superscript T means transposed. Superscripts $\boldsymbol{E}$, $\boldsymbol{D}$, $\boldsymbol{\varepsilon}$, and $\boldsymbol{\sigma}$ signify that these variables are held constant during the measurement of the tensor, *e.g.* in the first pair of equations we have s^E_{ijkl} is the elastic compliance tensor measured at constant electric field and κ^σ_{ik} is the dielectric permittivity at constant stress. For first pair of constitutive equations below illustrate the role of piezoelectric strain coupling to electric field with the piezoelectric tensor d. We have on the right hand side the variables associated with mechanical stress $\boldsymbol{\sigma}$ and electric field $\boldsymbol{E}$ in both equations. On left hand side the resulting values of elastic strain $\boldsymbol{\varepsilon}$ and $\boldsymbol{D}$ electric displacement, hence these equations are called the Strain-Electric displacement equations. In the first equation, the first and second terms on the right-hand side are the stress and the electric field contributions to the elastic strain. The second term is the piezoelectric converse coupling effect. In the second equation, the first and second terms on the right-hand side are the stress and electric field contributions to electric displacement. The first term is the piezoelectric direct coupling effect and the second is the classical relation for electric displacement for a dielectric crystal. The same logic applies to the other pairs of equations.

Piezoelectric strain to electric field coupling or Strain-Electric displacement equations with 'strain' piezoelectric tensor d

$$\begin{aligned} \varepsilon_{ij} &= s^E_{ijkl}\sigma_{kl} + d_{kij}E_k, & \boldsymbol{\varepsilon} &= \boldsymbol{s^E\sigma} + (\boldsymbol{d})^{\mathsf{T}}\boldsymbol{E} \\ D_i &= d_{ijk}\sigma_{ij} + \kappa^\sigma_{ik}E_k, & \boldsymbol{D} &= \boldsymbol{d\sigma} + \boldsymbol{\kappa^\sigma E} \end{aligned}$$

Piezoelectric stress to electric field coupling or Stress-Electric displacement equations with 'stress' piezoelectric tensor $\boldsymbol{e}$

$$\begin{aligned} \sigma_{ij} &= c^E_{ijkl}\varepsilon_{kl} - e_{kij}E_k, & \boldsymbol{\sigma} &= \boldsymbol{c^E\varepsilon} - \boldsymbol{e}^{\mathsf{T}}\boldsymbol{E} \\ D_i &= e_{ijk}\varepsilon_{kl} + \kappa^\varepsilon_{ik}E_k, & \boldsymbol{D} &= \boldsymbol{e\varepsilon} + \boldsymbol{\kappa^\varepsilon E} \end{aligned}$$

Piezoelectric electric field to stress coupling or Strain-Electric field equations with 'strain' piezoelectric tensor g

$$\begin{aligned} \varepsilon_{ij} &= s^D_{ijkl}\sigma_{kl} + g_{kij}D_k, & \boldsymbol{\varepsilon} &= \boldsymbol{s^D\sigma} + (\boldsymbol{g})^{\mathsf{T}}\boldsymbol{D} \\ E_i &= -g_{ijk}\sigma_{jk} + \beta^\sigma_{ik}D_k, & \boldsymbol{E} &= -\boldsymbol{g\sigma} + \boldsymbol{\beta^\sigma D} \end{aligned}$$

Piezoelectric electric field to strain coupling or Stress-Electric field equations with 'stress' piezoelectric tensor h

$$\begin{aligned} \sigma_{ij} &= c^D_{ijkl}\varepsilon_{kl} - h_{kij}D_k, & \boldsymbol{\sigma} &= \boldsymbol{c^D\varepsilon} - (\boldsymbol{h})^{\mathsf{T}}\boldsymbol{D} \\ E_i &= -h_{ijk}\varepsilon_{kl} + \beta^\varepsilon_{ik}D_k, & \boldsymbol{E} &= -\boldsymbol{h\varepsilon} + \boldsymbol{\beta^\varepsilon D} \end{aligned}$$

Now we have a set of 4 piezoelectric tensors, $\boldsymbol{d}$, $\boldsymbol{e}$, $\boldsymbol{g}$ and $\boldsymbol{h}$, which form two related sets $(\boldsymbol{d}, \boldsymbol{g})$ and $(\boldsymbol{e}, \boldsymbol{h})$, an illustration of their roles in the direct and converse effects is given by the square diagram in Figure 6B. We can also see the relation between $\boldsymbol{d}$ and $\boldsymbol{g}$ by writing them in a differential form with direct effect first and the converse second makes it clear they both are related in the direct effect to $\partial\sigma$ and in the converse effect to $\partial\varepsilon$. The differential form of the tensors is given by

$$
\begin{aligned}
d_{ijk} &= +\left(\frac{\partial D_i}{\partial \sigma_{jk}}\right)_E = +\left(\frac{\partial \varepsilon_{jk}}{\partial E_i}\right)_\sigma \\
g_{ijk} &= -\left(\frac{\partial E_i}{\partial \sigma_{jk}}\right)_D = +\left(\frac{\partial \varepsilon_{jk}}{\partial D_i}\right)_\sigma .
\end{aligned}
$$

Secondly, the relation between $\boldsymbol{e}$ and $\boldsymbol{h}$ are both related in the direct effect in the first relationship to $\partial\varepsilon$ and in the converse effect in the second relationship to $\partial\sigma$

$$
\begin{aligned}
e_{ijk} &= +\left(\frac{\partial D_i}{\partial \varepsilon_{jk}}\right)_E = -\left(\frac{\partial \sigma_{jk}}{\partial E_i}\right)_\varepsilon \\
h_{ijk} &= -\left(\frac{\partial E_i}{\partial \varepsilon_{jk}}\right)_D = -\left(\frac{\partial \sigma_{jk}}{\partial D_i}\right)_\varepsilon .
\end{aligned}
$$

The close relation of these two sets is also important for understanding their transformation between Voigt matrix and tensor notation and vice-versa. For transformation 3-index to 2-index for the tensors d_{ijk} and g_{ijk}

$$
\begin{aligned}
&d_{ijk} = d_{in} \text{ and } g_{ijk} = g_{in} \text{ with } i,j,k = 1,2,3 \text{ when } j = k, n = 1,2 or 3, \\
&d_{ijk} = \frac{1}{2} d_{in} \text{ and } g_{ijk} = \frac{1}{2} g_{in} \text{ with } i,j,k = 1,2,3 \text{ when } j \neq k, n = 4,5 or 6.
\end{aligned}
$$

and transformation 2-index to 3-index for the tensors d_{ijk} and g_{ijk}

$$
\begin{aligned}
&d_{in} = d_{ijk} \text{ and } g_{in} = g_{ijk} \text{ with } i,j,k = 1,2,3 \text{ when } j = k, n = 1,2 or 3, \\
&d_{in} = 2 d_{ijk} \text{ and } g_{in} = 2 g_{ijk} \text{ with } i,j,k = 1,2,3 \text{ when } j \neq k, n = 4,5 or 6,
\end{aligned}
$$

where for d_{ijk} and g_{ijk} the factor $\frac{1}{2}$ or 2 is due the conversions from Voigt matrix shear strain to tensor strains or vice-versa. These transformations are activated in `MTEX` by the option `DoubleConvention` in the tensor command.

For transformation 3-index to 2-index for the tensors e_{ijk} and h_{ijk}

$$
e_{ijk} = e_{in} \text{ and } h_{ijk} = h_{in}, \quad i,j,k = 1,2,3 n = 1,2,3,4,5,6
$$

and transformation 2-index to 3-index for the tensors e_{ijk} and h_{ijk}

$$
e_{in} = e_{ijk} \text{ and } h_{in} = h_{ijk}, \quad i,j,k = 1,2,3 n = 1,2,3,4,5,6
$$

where for e_{ijk} and h_{ijk} there are no correction factors. These transformations are activated in `MTEX` by the option `SingleConvention` in the tensor command.

The relationship between all $\boldsymbol{d}$, $\boldsymbol{e}$, $\boldsymbol{g}$ and $\boldsymbol{h}$ tensors provides a route for calculating one type of piezoelectric tensor from another as it is rare that publications quote coefficients of all 4 piezoelectric tensors.

$$
\begin{aligned}
d_{nkl} &= e^{\sigma}_{mn} g_{mkl} = e_{nij} s^{E}_{ijkl} & \quad \boldsymbol{d} &= \boldsymbol{e^{\sigma} g} = \boldsymbol{e s^{E}} \\
e_{nkl} &= e^{\varepsilon}_{mn} h_{mkl} = d_{nij} c^{E}_{ijkl} & \quad \boldsymbol{e} &= \boldsymbol{e^{\varepsilon} h} = \boldsymbol{d c^{E}} \\
g_{nkl} &= \beta^{\sigma}_{mn} d_{mkl} = h_{nij} s^{D}_{ijkl} & \quad \boldsymbol{g} &= \boldsymbol{\beta^{\sigma} d} = \boldsymbol{h s^{D}} \\
h_{nkl} &= \beta^{\varepsilon}_{mn} e_{mkl} = g_{nij} c^{D}_{ijkl} & \quad \boldsymbol{h} &= \boldsymbol{\beta^{\varepsilon} e} = \boldsymbol{g c^{D}}
\end{aligned}
$$

2.7 Standards for piezoelectric crystal properties

Over the years various conventions for the signs of physical properties of piezoelectric crystals have been proposed for crystals such as α-quartz, which has left- and right-handed forms. The best known conventions are the International Radio Engineers (IRE) standard published in 1949 (Brainerd et al.,1949) and the more recent Institute of Electrical and Electronic Engineering (IEEE) ANSI-IEEE 176 standard published in 1988 (http://www.ieee.org). Both are considered important industrial standards, but as can been seen from Table 1 the sign conventions for elastic and piezoelectric tensors for α-quartz are different. We have made Table 2 with all the values for right and left-handed α-quartz given in the IRE 1949 standard. If we know the values for d_{ijk} and c^{E}_{ijkl} from Table 2, then we calculate the coefficients for the other piezoelectric tensors ($\boldsymbol{e}$, $\boldsymbol{g}$ and $\boldsymbol{h}$) in self-consistent way using the relationships given above starting with $e_{nkl} = d_{nij}\ c^{E}_{ijkl}$.

In tensor notation this reduces to two independent non-zero coefficients for α-quartz with point group symmetry **32**

$$
\begin{aligned}
e_{111} &= d_{111}(c^{E}_{1111} - c^{E}_{1122}) + 2 d_{123} c^{E}_{1123} = e_{11}, \\
e_{123} &= d_{111} c^{E}_{1123} + d_{122} c^{E}_{2223} + 2(d_{123} c^{E}_{2323}) = e_{14}.
\end{aligned}
$$

In Voigt matrix notation this can be written as

$$
e_{11} = d_{11}(c^{E}_{11} - c^{E}_{12}) + d_{14} c^{E}_{14}, e_{14} = d_{11} c^{E}_{14} + d_{12} c^{E}_{24} + d_{14} c^{E}_{44}.
$$

Similarly for the g_{nkl} tensor we can write

$$
g_{nkl} = \beta^{\sigma}_{mn} d_{nkl},
$$

where β^{σ}_{mn} is inverse of κ^{σ}_{mn} given in table 1, so that

$$
g_{111} = (\kappa^{\sigma}_{11})^{-1} d_{111} = g_{11}, g_{123} = (\kappa^{\sigma}_{11})^{-1} d_{123} = g_{14}/2.
$$

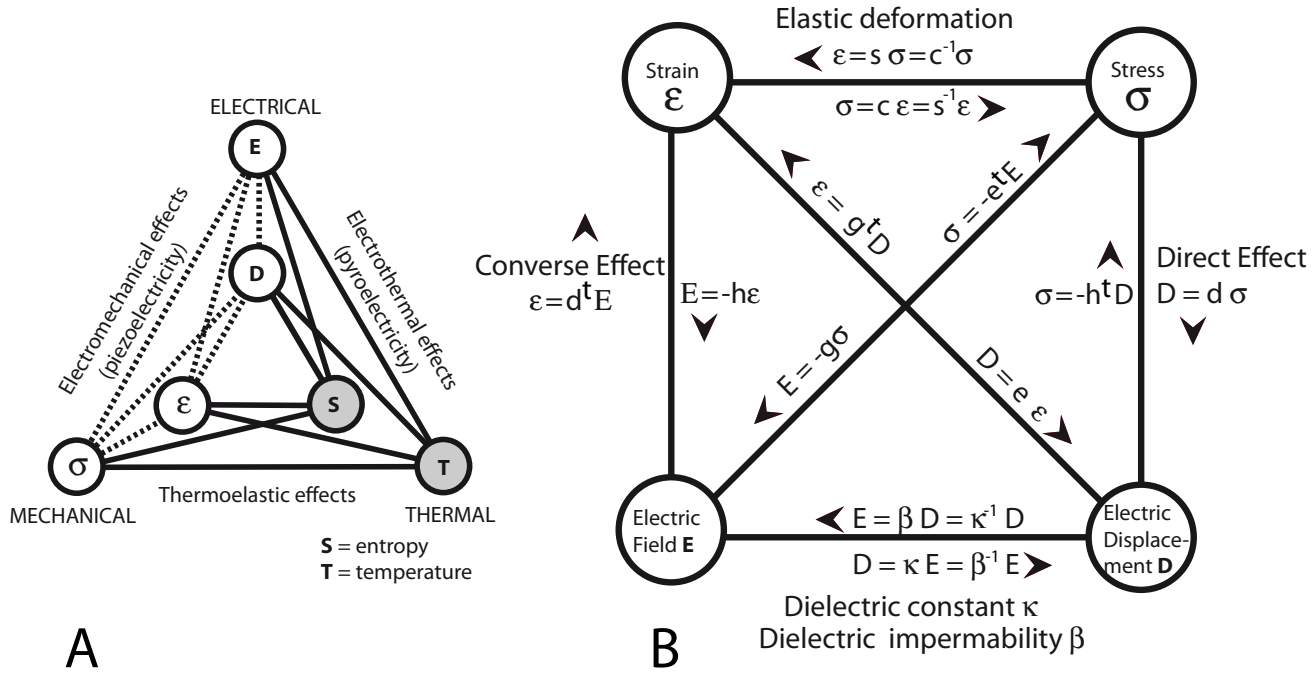

Figure 6: Interaction between variables : A) The Heckmann triangle (left) shows the complete set of thermodynamical variables, the variables chosen for constitutive equations are in the white circles and the constant variables (entropy and temperature) in circles with grey shading.
B)The interaction square (right) with strain, stress, electric displacement and electric field variables at constant entropy and temperature. The piezoelectric tensors $\boldsymbol{d}$, $\boldsymbol{e}$, $\boldsymbol{g}$ and $\boldsymbol{h}$ in the direct effect are marked with arrows towards bottom and in the converse effect towards to top.

For the tensor $h_{nkl} = \beta^{\boldsymbol{\varepsilon}}_{mn} e_{nkl}$, although we do not have a value for $\varepsilon^{\boldsymbol{\varepsilon}}_{mn}$ in table 3, we can calculate the necessary correction from

$$\kappa^{\sigma}_{mn} - \kappa^{\boldsymbol{\varepsilon}}_{mn} = d_{nkl} e_{mkl},$$

where

$$\kappa^{\sigma}_{11} - \kappa^{\boldsymbol{\varepsilon}}_{11} = 0.57 \times 10^{-12} \mathrm{mf}^{-1},$$

which gives $\kappa^{\boldsymbol{\varepsilon}}_{11} = 39.74 \times 10^{-12} \mathrm{mf}^{-1}$, and hence

$$h_{111} = (\kappa^{\boldsymbol{\varepsilon}}_{11})^{-1} e_{111} = h_{11},$$
$$h_{123} = (\kappa^{\boldsymbol{\varepsilon}}_{11})^{-1} e_{123} = h_{14}.$$

Using this method we have checked the coherency of the sign conventions of IRE 1949 and IEEE 1987 standards for the four piezoelectric tensors, both are internally consistent and in agreement with the equations above. A further consistency check was made by LePage et al.(2002) on the sign of the elastic stiffness coefficient c_{14} for right-handed α-quartz using *ab initio* methods and they found that the sign was negative, which can only be consistent with the IRE 1949 standard (Table 2). Hence we have decided to use IRE 1949 standard in this paper and most recent published values of piezoelctric tensors for α-quartz by Ogi et al.(2006).

2.8 Elastic wave propagation

For the wave propagation in an infinite elastic piezoelectric medium the appropriate independent variables are the strain (ε) and the electric field (E), which define the constitutive equations coupling the elastic (acoustic) and electromagnetic waves caused by a mechanical vibration. This choice of constitutive equations is some times called the piezoelectric stress equations due to the presence of the e_{ijk} tensor. There are five plane wave coupled solutions in a piezoelectric medium, three elastic and two electromagnetic (e.g. Auld, 1990). Detailed analysis shows that the effects of piezoelectric coupling of elastic and electromagnetic planes waves in infinite media are negligible in comparison with the influence of the quasi-static electric field. The velocity of elastic (acoustic) waves is approximately five orders of magnitude lower than electromagnetic waves. Hence it is only the quasi-static part of the electric field that affects the propagation of elastic waves. The quasi-static electric approximation neglects the rotational part (i.e. the magnetic field B part) of the electromagnetic field ($-\nabla \times E = \partial B/\partial t = 0$ and $-\nabla . E = \rho/\varepsilon_0$, where t is time, ρ is total charge density, ε_0 is permittivity of a vacuum) and retains only the scalar electric field ($E = -\nabla\Phi$, where Φ is the electric potential). The quasi-static electric approximation introduces insignificant errors for elastic wave propagation (Auld,1990). In what follows we use explicit formulations for the strain tensor, where u is the displacement

$$\varepsilon_{kl} = \frac{1}{2}\left(\frac{\partial u_l}{\partial x_k} + \frac{\partial u_k}{\partial x_l}\right),$$

the quasi-static electric field lines are perpendicular to equipotential surfaces in $E_k = -\left(\frac{\partial \Phi}{\partial x_k}\right)$ to develop a form of the constitutive equations suitable for the study of elastic wave propagation

$$\sigma_{ij} = c^E_{ijkl}\varepsilon_{kl} - e_{kij}E_k = c^E_{ijkl}\frac{\partial u_l}{\partial x_k} + e_{kij}\frac{\partial \Phi}{\partial x_k}$$
$$D_j = e_{jkl}\varepsilon_{kl} + \kappa^{\varepsilon}_{jk}E_k = e_{jkl}\frac{\partial u_l}{\partial x_k} - \kappa^{\varepsilon}_{jk}\frac{\partial \Phi}{\partial x_k}$$

If we ignore the effect of gravity on Newton's second law an equation of motion can be written as displacement u_i as function of time with $\frac{\partial \sigma_{ij}}{\partial x_j} = \rho\frac{\partial^2 u_i}{\partial t^2}$. From Maxwell's electrostatic equation for an insulator we have that the divergence is $\frac{\partial D_j}{\partial x_j} = 0 (j = 1, 2, 3)$, that is flux entering any element of space is exactly balanced by that leaving it. Substitution of the modified constitutive equations above into Newton's and Maxwell's equations yields the following differential equations,

$$\frac{\partial \sigma_{ij}}{\partial x_j} = \rho\frac{\partial^2 u_i}{\partial t^2} = c^E_{ijkl}\frac{\partial^2 u_l}{\partial x_j \partial x_k} + e_{kij}\frac{\partial^2 \Phi}{\partial x_j \partial x_k}$$
$$\frac{\partial D_j}{\partial x_j} = 0 = e_{jkl}\frac{\partial^2 u_l}{\partial x_j \partial x_k} - \kappa^{\varepsilon}_{jk}\frac{\partial^2 \Phi}{\partial x_j \partial x_k}$$

The first equation corresponds to the equation of motion for non-piezoelectric elastic medium with the addition of the second term on the right-hand side that adds to the elastic stiffness term. The second equation is related to the electrical displacement field, which has a divergence of zero.

We require the solution for the displacement of monochromatic plane wave that can be described by any harmonic form as a function of time, for example $u_k = A_k \exp i(\omega t - v_i.x_i)$ where ω is the angular frequency, A_k is the amplitude, v_i is wave vector and x_i is the position vector. The solution of the system of dynamic equations for plane waves are following equations (e.g. Royer and Dieulesaint, 1996)

$$\rho V^2 p_i = \Gamma_{il}p_l + \gamma_i \Phi$$
$$0 = \gamma_l p_l - \kappa \Phi$$

with

$$\Gamma_{il} = c^E_{ijkl}n_j n_k, \quad \gamma_i = e_{kij}n_j n_k \text{ and } \kappa = \kappa^{\varepsilon}_{jk}n_j n_k,$$

where V is the wave velocity and p_i is the particle movement or polarization direction. Γ_{il} is the familiar symmetric Christoffel tensor of a non-piezoelectric material, the other two terms γ_i and κ are specific quantities related to the piezoelectric properties, and all three the depend on the direction of propagation (n_i). The scalar factor Φ of electric potential in both equations on the left-hand side may be removed by division and we find an equation

similar to the Christoffel equation for an anisotropic elastic medium plus the $\frac{\gamma_i\gamma_l}{\kappa}$ term (Sirotin and Shaskolskaya, 1982; Royer and Dieulesaint, 1996)

$$\rho V^2 p_i = \left(\Gamma_{il} + \frac{\gamma_i\gamma_l}{\kappa}\right) p_l$$

We can now write the stiffened Christoffel tensor $\bar{\Gamma}_{il}$ of a piezoelectric material as

$$\bar{\Gamma}_{il} = \Gamma_{il} + \frac{\gamma_i\gamma_l}{\kappa}$$

Alternatively we write the piezoelectric stiffened elastic constants as (Ikeda, 1990; Auld,1990)

$$\bar{c}^E_{ij} = c^E_{ij} + \frac{(e_{im}n_m)(e_{mj}n_m)}{\kappa^\varepsilon_{kl}n_k n_l} = \boldsymbol{c}^E + \frac{(\boldsymbol{e}^\mathsf{T}\cdot\boldsymbol{n})(\boldsymbol{e}\cdot\boldsymbol{n})}{\boldsymbol{n}^\mathsf{T}\cdot\boldsymbol{\kappa}^\varepsilon\cdot\boldsymbol{n}}$$

and hence an alternative formulation of the stiffened Christoffel tensor,

$$\bar{\Gamma}_{il} = \bar{c}^E_{ijkl}n_j n_k = \boldsymbol{n}\cdot\bar{\boldsymbol{c}}^E\cdot\boldsymbol{n}$$

However, as pointed out by Royer and Dieulesaint (1996) the piezoelectric stiffened elastic constants are not elastic constants in the conventional sense because of the additional piezoelectric terms which are themselves dependent on the propagation direction. Sirotin and Shaskolskaya (1982) and Royer and Dieulesaint (1996) suggest using the velocities calculated from $\bar{\Gamma}_{il} = \Gamma_{il} + \frac{\gamma_i\gamma_l}{\kappa}$ for practical applications. However we favour using the method of Ikeda (1990) and Auld (1990), as this formulation conserves the full tensor notation and only requires the calculation of modified stiffened elastic constants for each propagation direction, which is used in a standard Christoffel tensor calculation. From either formulation we see that the Christoffel tensor is symmetric and therefore three velocities have orthogonal polarizations as in a non-piezoelectric material. From the equation of the displacement of monochromatic plane wave and requirements of Maxwell's equations for quasi-static electrical fields it can be shown that E is parallel (longitudinal) to and D associated with electric power flow is perpendicular (transverse) to the direction of propagation (n_i) in all cases (Auld, 1990; Ikeda, 1990), and hence each plane wave has constant electric potential.

3 Applications

3.1 Elastic wave propagation

To confirm the validity of our `MTEX` code for calculating the elastic wave speed in piezoelectric crystals we have plotted the slowness (1/wave-speed) surfaces of two crystals with a well-known strong coupling behaviour, lithium niobate ($LiNbO_3$) (Warner et al.,1967) point group **3m** and zincite (ZnO) **6mm** (Kobiakov,1980). Coupling behaviour is detected when the elastic wave-speed calculated using the full piezoelectric formulation given above

with stiffened elastic constants is higher than the classical elastic calculation using the ordinary stiffness constants. The plots the most frequently used in crystal physics to illustrate the effect of coupling are 2D sections of the slowness surface normal to one of the tensor reference directions (X, Y or Z). Figure 7A shows the the plot for lithium niobate normal to X direction (a-axis) where the S waves with their polarization normal to X show a strong decrease in slowness (increase in wave-speed) for porpagation directions near the Y-axis. In contrast the S waves with their polarization parallel to X show no coupling effect. The P waves also exhibit a coupling effect in most propagation directions in the YZ section. Zincite is hexagonal and it elastic properties have transverse isotopic symmetry about the c-axis, so that any plane normal to the c-axis ($\|Z$-axis) will display the same slowness surfaces. In figure 7B we have plotted the the slowness surfaces normal to the Y direction, the P and S wave with polarization normal to Y show a reduction in slowness (increase in wave-speed) typical of a coupling effect. The S wave with polarization parallel to Y shows no coupling effect. Both figures of slowness surfaces agree with previously published plots by Auld (1990) and Royer and Dieulesaint (1996). `MTEX` can also plot the wave speeds and polarization in various pole figure plots, which allows more complete understanding of the coupling effect.

We investigate the effect of piezoelectric coupling on elastic wave speeds in α-quartz. In right- and left-handed crystals the P, S_1 and S_2 wave speeds are exactly the same along the c-axis with 6.3144, 4.6884 and 4.6884 km/s with or without piezoelectric coupling. Given that the pizeoelectric tensors have zero values along the c-axis (e.g. Figure 2) this is to be expected. A potentially stronger coupling may occur along the a-axes in the basal plane where the piezoelectric tensors have their highest values. For example the P, S_1 and S_2 wave-speed along the positive and negative a-axes are higher with coupling by 0.006, 0.07 and 0.6 % than an elastic calculation without coupling. These results are confirmed by the plot of the slowness in the basal plane for right- (Figure 7A) and left-handed (Figure 7B) quartz, the piezoelectric coupling has almost no effect on the the elastic wave speeds in α-quartz.

The effect of coupling on the elastic wave speed anisotropy is complex, for Lithium Niobate, which clearly has the strongest coupling we have considered the P-wave (AVp) and S-wave (AVs) anisotropy with piezoelectric coupling is AVp=11.0 % and AVs=16.9 %, where as for the elastic case with no coupling AVp= 12.5 % and AVs=17.5 %. For Zincite with intermediate piezoelectric coupling is AVp=7.1 % and AVs=12.0 %, where as for the elastic case with no coupling AVp= 1.8 % and AVs=6.6 %. Quartz with very weak piezoelectric coupling AVp=27.7 % AVs=43.1 % for with and without coupling. So the effect of piezoelectric coupling on wave speed anisotropy depends on specific 3D velocity distribution induced by the coupling. For the case of Zincite the anisotropy is multiplied by 3 for AVp and 2 for AVs.

3.2 Polycrystalline quartz vein

Previous measurements on a quartz mylonite by Bishop(1981) showed a piezoelectric effect of about 1.5% of the single crystal, where as a quartz vein sample measured by Ghomshei

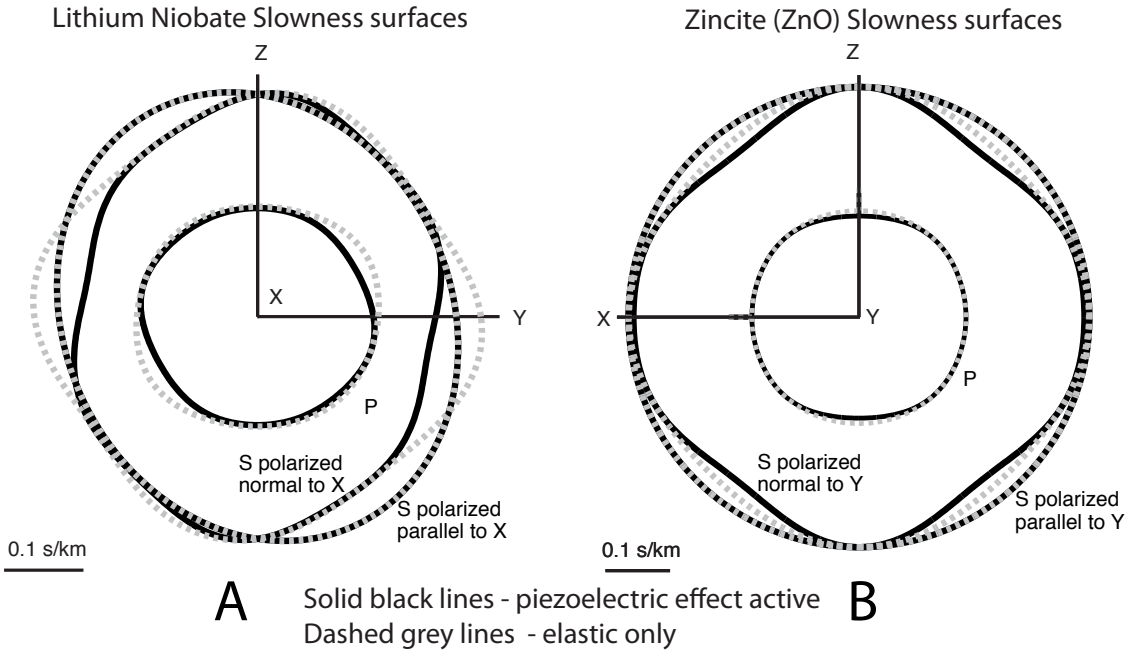

Figure 7: Slowness surfaces with A : Lithium Niobate (**3m**) and B : Zincite (**6mm**), where $\mathbf{X} = \mathbf{a}[2\bar{1}\bar{1}0]$,$\mathbf{Y} = \mathbf{m}[01\bar{1}0]$,$\mathbf{Z} = \mathbf{c}[0001]$

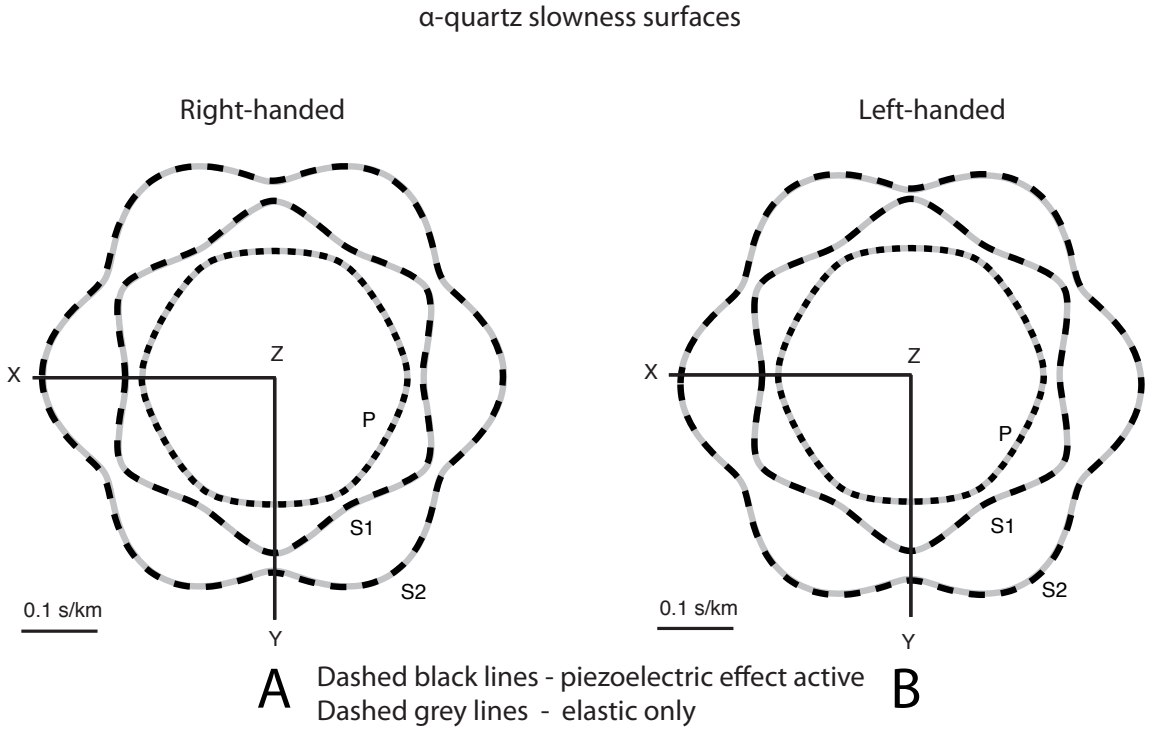

Figure 8: Slowness surfaces for α-quartz (**32**) : A) right-handed and B) left-handed, where $\mathbf{X} = \mathbf{a}[2\bar{1}\bar{1}0]$,$\mathbf{Y} = \mathbf{m}[01\bar{1}0]$,$\mathbf{Z} = \mathbf{c}[0001]$

et al.(1988) showed a maxmium effect of 7% of the single crystal, and various studies from the Russian literature confirm that quartz veins frequently have a strong piezoelectric effect (Parkhomenko, 1981). Hence we selected a quartzite that was probably originally a quartz vein from the Tongue quartzite (Moine Thrust zone, Eriboll, N. Scotland). The sample has been previously studied by Lloyd *et al.*(1987) and Mainprice et al.(1993). A total of the 382 ECPs were recorded using a CamScan S4 SEM fitted with electron beam rocking coils. The patterns were indexed manually or by computer aided techniques by G.E. Lloyd at Leeds University. The 382 individual orientations have been indexed as right-handed crystals with convention that the positive rhomb **r** is a stronger reflection than the negative rhomb **z** (see Donnay and LePage 1978). The original ECP indexing solutions have been converted to Bunge Euler angles and imported into `MTEX` using the EBSD generic import filter to create an object containing the individual orientation data. The orientation distribution function for right-handed indexed quartz calculated using default de la Vallee Poussin kernel with halfwidth of 10 degrees corresponding a harmonic expansion of 28. A list of pole figures was defined using the command Miller and the pole figures plotted with command plot.

```
% create an EBSD variable containing the data
ebsd = loadEBSD(fname,CS,SS,'interface','generic',...
  'ColumnNames',{'phi1' 'Phi' 'phi2'},'Bunge')
% Calculate an ODF of right-hand index quartz
odf_qtz_rh = calcODF(ebsd('Quartz'),'HALFWIDTH',10*degree)
% quartz pole figure list
% c(00.1),a(2-1.0),m(10.0),r(10.1),z(01.1) quartz
h_qtz = [Miller(0,0,0,1,CS),Miller(2,-1,-1,0,CS),...
Miller(1,0,-1,0,CS),Miller(1,0,-1,1,CS),Miller(0,1,-1,1,CS)];
% antipodal
plotpdf(odf_qtz_rh,h_qtz,'resolution',5*degree,'contourf','antipodal')
```

To plot inverse pole figures (IPFs) the specimen directions must be defined. In the simplest cases one can use the predefined ones in Cartesian specimen coordinates called xvector, yvector and zvector. For specific specimen directions you can use the command `vector3d`

```
polar_angle = 60*degree;
azimuth_angle = 45*degree;
r = vector3d('polar',polar_angle,azimuth_angle);
```

for example we want defined two positions in pole figure coordinates labelled **A** and **P**;
i) **A** is an orientation in the $\mathbf{a}\{2\bar{1}\bar{1}0\}$ pole figure with high values in multiples of uniform distribution is at polar angle 90° and azimuth 130°,
ii) **P** is an orientation in the $\mathbf{z}\{01\bar{1}1\}$ pole figure with a high value in multiples of uniform distribution is at polar angle 90° and azimuth 220°.
The inverse pole figures corresponding to specimen directions **A** and **P** can be ploted with command `plotipdf`.

```
% define pole figure directions A and P
polar_angle_A = 90*degree;
azimuth_angle_A = 130*degree;
polar_angle_P = 90*degree;
```

```
azimuth_angle_P = 220*degree;
r = [vector3d('polar',polar_angle_A,azimuth_angle_A), ...
     vector3d('polar',polar_angle_P,azimuth_angle_P)];
% plot inverse pole figure
plotipdf(odf_qtz_rh,r,'earea','complete',...
'resolution',5*degree,'contourf','antipodal')
```

From these compact commands we can plot the pole figures and inverse pole figures with the 'podal' default setting or the option 'antipodal'. In MTEX 'podal' means that vectors with positive and negative ends are treated as such, and will require in general to be plotted on the sphere or on two hemispheres. Other workers have called the 'podal' operation to be 'polar' directions or vectors. The option 'antipodal' will treat a vector as unsigned 'axis' also known as 'non-polar' direction. All the data plotted with the 'antipodal' option can be plotted in one hemisphere.

In Figure 9 the classical pole figures used for quartz have been plotted as podal plots. The a-axis is the only axis that has polarity in α-quartz. In the IPF (Figure 10) of the specimen direction 'A' the podal plot has 3-fold symmetry as you would expect for α-quartz. The highest densities in the 'A' direction IPF correspond to $+\mathbf{a}\{2\bar{1}\bar{1}0\}$ and its symmetry equivalents. The IPFs for the 'P' specimen direction are almost identical between upper and lower hemispheres, with high densities parallel to the poles of $\mathbf{m}\{10\bar{1}0\}$ and $\mathbf{z}\{01\bar{1}1\}$. Notice that the 'P' direction IPF also has a slightly imperfect 3-fold symmetry.

The next step is to calculate the piezoelectric tensor $\boldsymbol{d}$ for our ideal right-handed α-quartz aggregate. Mainprice et al.(2011) describe in some detail the methods for calculating the average properties of aggregates for symmetric 2^{nd} and 4^{th} physical property tensors. Here we will recall that the Voigt and Reuss averages in MTEX have been developed for individual orientations (ECP, EBSD, U-stage etc) as simple summations and via the ODF by numerical integration or via the ODF Fourier coefficients. The route via the Fourier coefficients is particularly efficient and can be applied to ODFs of single orientations or derived from pole figure inversion. The one caveat is that we have 4 piezoelectric tensors and their transpose for the direct and converse piezoelectric effects respectively (see Figure 5), but the tensors are not symmetric and hence these tensors inverse like elastic stiffness tensor has its inverse, which is the elastic compliance tensor. Hence we can calculate the Voigt average tensor using the piezoelectric tensors, but not the Reuss average as this would require the inverse piezoelectric tensors, as they do not exist. The other caveat in piezoelectric properties is that there is always some coupling as described by the constitutive equations above, a simple Voigt average clearly does not take this into account. Despite these limitations various studies have shown that Voigt average is in reasonable agreement (within 10 %) with experimental results and variational Hashin-Shtrikman upper bound (e.g. Li and Dunn, 2001; Wan et al., 2012).

We start with the case that we have individual orientation data $g_m, m = 1, \ldots, M$, ECP measurements, and volume fractions $V_m, m = 1, \ldots, M$. Then the Voigt (1887,1910) effective piezoelectric properties of aggregates are those defined by assuming that the induced tensor (in broadest sense including vectors *e.g.* electric polarization vector for the direct effect and elastic strain tensor for converse effect) field is everywhere homogeneous or

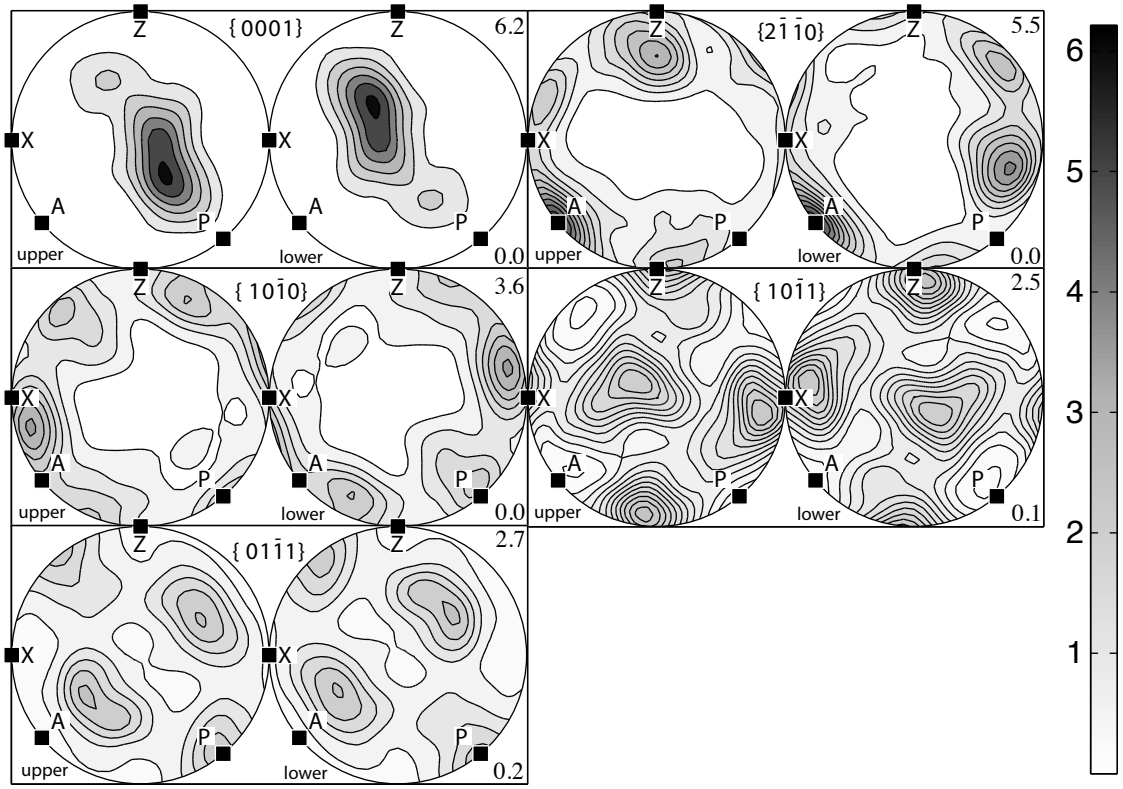

Figure 9: Polefigure plots of $\mathbf{c}\{0001\}$,$\mathbf{a}\{2\bar{1}\bar{1}0\}$,$\mathbf{m}\{10\bar{1}0\}$,$\mathbf{r}\{10\bar{1}1\}$,$\mathbf{z}\{01\bar{1}1\}$. The figure was generated using the 'complete' `MTEX` option where positive and negative crystallographic vectors kept in their appropriate original orientations. The 'complete' plot reveals that thee is a strong preference for one $\mathbf{a}\{2\bar{1}\bar{1}0\}$ pole. X is lineation and Z is the normal to the foliation. **A** marks the maximum in the $\mathbf{a}\{2\bar{1}\bar{1}0\}$ pole figure. **P** marks a high density in $\mathbf{m}\{10\bar{1}0\}$ and $\mathbf{z}\{01\bar{1}1\}$ pole figures. Upper hemisphere on the left and lower hemisphere plots in right. Notice that upper and lower hemisphere plots are rotated by 180 degrees, except for the $\mathbf{a}\{2\bar{1}\bar{1}0\}$ pole figure as positive and negative directions are not equivalent.

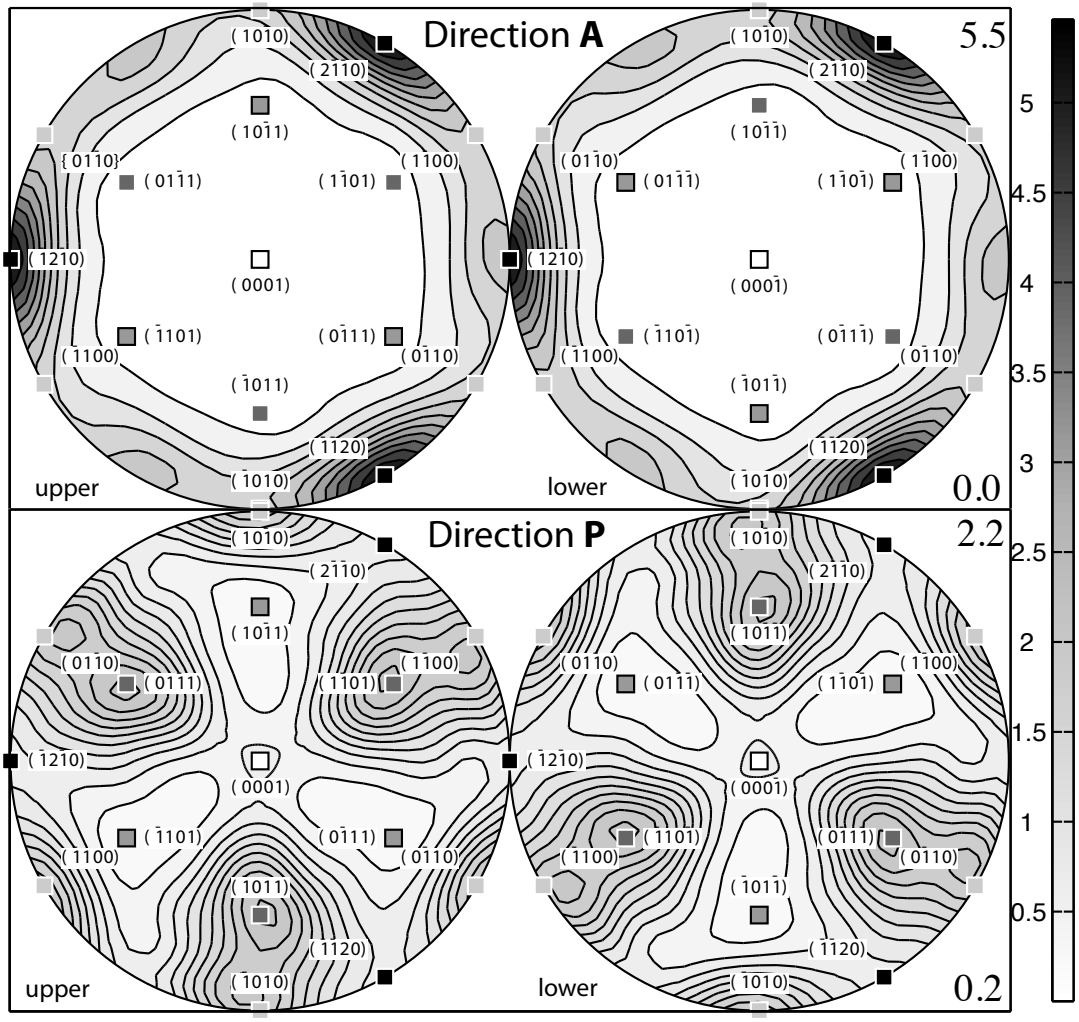

Figure 10: The inverse pole figures (IPFs) of the specimen directions **A** (top row) and **P** (bottom row) marked on the pole figures in Figure 9. Left is upper hemisphere and right is lower hemisphere plots. The crystallographic directions of the pole figures on marked on the IPFs. On the A-direction IPFs the with 'complete' option clearly shows preference for $+\mathbf{a}\{2\bar{1}\bar{1}0\}$ preferred orientation with multiples of a uniform distribution reaching 5.5. The P-direction IPFs the high densities (*ca* 2.2) for $\mathbf{m}\{10\bar{1}0\}$ and $\mathbf{z}\{01\bar{1}1\}$ directions.

constant, *i.e.*, the induced tensor at every position is set equal to the macroscopic induced tensor of the specimen. The Voigt average specimen effective piezoelectric tensor $\langle d \rangle^{\text{Voigt}}$ is defined by the volume average of the individual tensors $d(g_m^c)$ with crystal orientations g_m^c and volume fractions V_m,

$$\langle d \rangle^{\text{Voigt}} = \sum_{m=1}^{M} V_m d(g_m^c).$$

To do a simple summation Voigt average for piezoelectric tensor $\boldsymbol{d}$ we used the command calcTensor. We previously defined the tensor $\boldsymbol{d}$ for right-handed α-quartz, we can do the same for the left-handed α-quartz and calculate the tensors for both handedness cases.

```
% Enter Piezoelectric (strain) tensor (d_ij) as (3 by 6) matrix
% Md line by line in pC/N
% Ogi, H., Ohmori, T. Nakamura, N. and Hirao M. (2006) RH alpha-quartz
% LH alpha-quartz d11 = +1.9222  d14 = +0.1423
Md_LH =[[+1.9222   -1.9222    0     +0.1423    0          0    ];...
    [   0          0         0        0       -0.1423    -3.8444];...
    [   0          0         0        0         0          0    ]];
d_LH_quartz = tensor(Md_LH,cs_Tensor,'rank',3,'propertyname',...
 'LH piezoelectric strain tensor','unit','pC/N','DoubleConvention')
%
% Voigt average for EBSD for right- and left-handed  alpha-quartz
%
d_RH_Voigt_Tongue_Quartzite = ...
    calcTensor(ebsd('Quartz'),d_RH_quartz,'Voigt')
d_LH_Voigt_Tongue_Quartzite = ...
    calcTensor(ebsd('Quartz'),d_LH_quartz,'Voigt')
```

```
d_RH_Voigt_Tongue_Quartzite = tensor (show methods, plot)
  propertyname    : RH piezoelectric strain tensor
  rank            : 3 (3 x 3 x 3)
  doubleConvention: true

  tensor in compact matrix form: *10^-2
  -8.761   23.593  -14.832   -6.251  -57.522  -23.927
  -13.01   -2.634   15.644   56.003    7.005   42.088
 -30.721   29.961    0.76    29.195  -24.565    2.078

d_LH_Voigt_Tongue_Quartzite = tensor (show methods, plot)
  propertyname    : LH piezoelectric strain tensor
  rank            : 3 (3 x 3 x 3)
  doubleConvention: true

  tensor in compact matrix form: *10^-2
   8.761  -23.593   14.832    6.251   57.522   23.927
   13.01    2.634  -15.644  -56.003   -7.005  -42.088
  30.721  -29.961    -0.76  -29.195   24.565   -2.078
```

From the results one can see that the Voigt polycrystal average gives the same magnitudes, but the positive and negative signs are opposite between the right- and left-hand

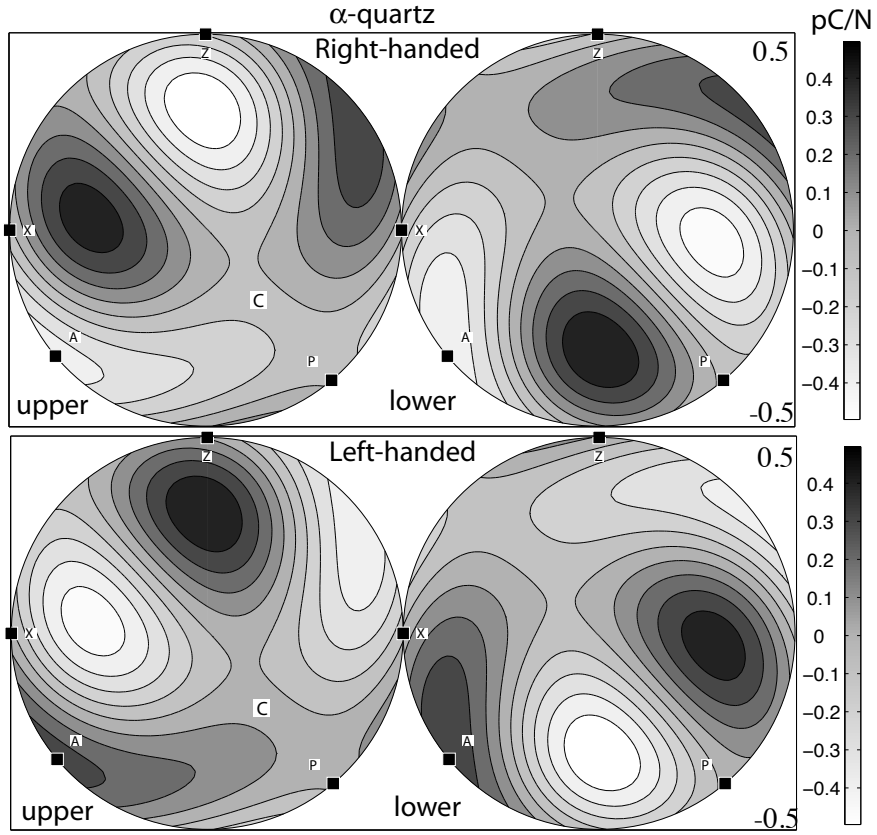

Figure 11: The pole figures of the Voigt average for piezoelctric strain tensor $\boldsymbol{d}$ assuming all the crystals are right-handed (top) with upper (left) and lower(right) hemisphere projections. Below assuming all the crystals are left-handed. Both right- and left-handed show extreme values near **A**, but the distribution is clearly 3-dimensional as shown by the upper (left) and lower(right) hemisphere projections with approximate 3-fold symmetry associated with the strong c-axis maximum near **C** in the upper hemisphere. X is lineation and Z is the normal to the foliation.**N.B.** the maximum magnitude is $\pm$ 0.5 pC/N that is 26% of the single crystal.

results. In fact just as they are in right- and left-hand single crystal tensors $\boldsymbol{d}$. So if we add right-handed single crystal tensor $\boldsymbol{d}$ to left-handed single tensor the result is a zero-values tensor, or in other words no piezoelectric effect. This is a situation that occurs in a single crystal if it is twinned with Brazil law where the host is for example right-handed and then the twin will be left-handed or vice-versa. Brazil twins are called 'optical' twins and Dauphiné twins are called 'electrical' twins (Frondel, 1962) in the piezoelectric oscillator-plate industry because they can be detected optically and electrically respectively. As pointed by Donnay and Le Page (1975) both Brazil and Dauphiné twins reverse the polarity of the two-fold a-axes and degrade the electrical properties of the crystals, where as only Brazil twin reverses optical activity along the c-axis. In the same way if we imagined a quartz aggregate with equal volumes of right-handed and left-handed crystals there would be no piezoelectric effect if the aggregate has topological electrical connections of all the quartz crystals. However, it should be recalled that in general the frequency of right- and left-handed quartz 49.5% and 50.5% respectively form a total of 7335 single crystals reported by Frondel (1962) based on several studies, hence both forms are equally likely to occur. We can plot the results for right-handed and left-handed aggregates for Voigt averages of the $\boldsymbol{d}$ tensor using the `plot` command, see Figure 11.

```
% pole figure representation of d'111 the longitudinal
% pizezoelectric surface
plot(d_RH_Voigt_Tongue_Quartzite,'complete')
colorbar
% Structural reference Z-X frame and labels A and P
annotate(r_ZXAP,'label',{'Z','X','A','P'},'backgroundcolor',...
    'w','FontSize',18)
% Grey scaled plots for publications
mtexColorMap white2black
```

Another important case to consider is the uniform crystallographic distribution and its effect on piezoelectric properties. In the case that the texture is given by an ODF f, which may originate from texture modelling (Bachmann et al., 2010), pole figures inversion (Hielscher & Schaeben, 2008) or density estimation from EBSD data (Hielscher et al., 2010), or the present case of a uniform ODF using the `MTEX` command `uniformODF`.

The Voigt average $\langle d \rangle^{\text{Voigt}}$ of a tensor d given an ODF f is defined by the integral

$$\langle d \rangle^{\text{Voigt}} = \int_{\text{SO(3)}} d(g) f(g) \, \mathrm{d}g. \tag{1}$$

Next the ODF can be expressed as an expansion into generalized spherical harmonics of the form

$$f(g) = \sum_{\ell=0}^{r} \sum_{k,k'=-\ell}^{\ell} \hat{f}(l,k,k') D_{kk'}^{\ell}(g).$$

The Fourier method uses the expansion of the rotated tensor into generalized spherical harmonics, $D_{kk'}^{\ell}(g)$. Let $d_{i_1,\ldots,i_r}$ be an piezoelectric tensor $\boldsymbol{d}$ of rank $r = 3$. Then it is well known (*cf* Bunge 1969, Ganster and Geiss, 1985, Mainprice and Humbert, 1994,

Morris, 2006) that the rotated tensor $d_{i_1,\dots,i_r}(g)$ has an expansion into generalized spherical harmonics up to order r,

$$d_{i_1,\dots,i_r}(g) = \sum_{\ell=0}^{r} \sum_{k,k'=-\ell}^{\ell} \hat{d}_{i_1,\dots,i_r}(l,k,k') D^{\ell}_{kk'}(g). \tag{2}$$

The explicit calculations of the coefficients $\hat{d}_{i_1,\dots,i_r}(l,k,k')$ are given in the Appendix of Mainprice et al.(2011)

The average tensor with respect to this ODF can be computed using the formula

$$\begin{aligned}\frac{1}{8\pi^2}\int_{\mathrm{SO}(3)} d_{i_1,\dots,i_r}(g) f(g) &= \frac{1}{8\pi^2}\int_{\mathrm{SO}(3)} d_{i_1,\dots,i_r}(g)\overline{f(g)}\,\mathrm{d}g \\ &= \sum_{\ell=0}^{r} \frac{1}{2\ell+1} \sum_{k,k'=-\ell}^{\ell} \hat{d}_{i_1,\dots,i_r}(l,k,k')\overline{\hat{f}(l,k,k')}.\end{aligned}$$

MTEX by default uses the Fourier approach for ODFs as compared to the approach using a quadrature rule it is much faster and independent of any discretization. The latter one is applied only in those cases when MTEX cannot determine the Fourier coefficients of the ODF in an efficient manner. Until now only the Bingham orientation distributions have this problem. All the necessary calculations are done automatically, including the correction for different crystal and tensor reference frames.

To calculate the Voigt average using an ODF with Fourier method you obtain the most accurate results (without bias) using the Dirichlet kernel with a bandwidth equal to the rank of the tensor property, for piezoelectric tensors with a bandwidth of three.

```
% Dirichlet kernel with Band-width = 3
K_Dirichlet = kernel('Dirichlet','bandwidth',3)
% Calculate the uniform ODF with alpha-quartz
% crystal symmetry (CS) and triclinic sample symmetry (SS)
Uniform_Quartzite_Odf = uniformODF(CS,SS,'kernel',K_Dirichlet)
% Voigt averages for RH and LH-quartz with uniform ODF
d_RH_Voigt_Uniform_Quartzite = ...
    calcTensor(Uniform_Quartzite_Odf,d_RH_quartz,'Voigt')
d_LH_Voigt_Uniform_Quartzite = ...
    calcTensor(Uniform_Quartzite_Odf,d_LH_quartz,'Voigt')
```

```
d_RH_Voigt_Uniform_Quartzite = tensor (show methods, plot)
  rank: 3 (3 x 3 x 3)

  tensor in compact matrix form:
 0 0 0 0 0 0
 0 0 0 0 0 0
 0 0 0 0 0 0

d_LH_Voigt_Uniform_Quartzite = tensor (show methods, plot)
  rank: 3 (3 x 3 x 3)
```

```
 tensor in compact matrix form:
0 0 0 0 0 0
0 0 0 0 0 0
0 0 0 0 0 0
```

Of course the results are the same for both right- and left-handed quartz with zero tensor $\boldsymbol{d}$ and no piezoelectric effect. So for enantiomorphic crystal like α-quartz there are two ways of obtaining no piezoelectric effect, equal volumes of right- and left-handed crystals with the same ODF or a uniform distribution of crystal orientations. In addition for the case of α-quartz both Brazil and Dauphiné twins will reduce the piezoelectric effect. For all aggregates piezoelectric crystals a uniform distribution of crystal orientations will result in no piezoelectric effect. Clearly the strategy for piezoelectric polycrystalline ferroelectric ceramics (e.g. lead zirconate titanate $PbZr_{1-x}Ti_xO_3$ Newnham, 2005) is to optimise the *ODF* to get the desired piezoelectric effect by various electrical and mechanical processes, which is referred to as poling. In geological samples like quartzites the maximum piezoelectric effect will occur if all crystals are of one handedness (*e.g.* right-handed) and the ODF is as close as possible to a single crystal, that is the point maximum for the *c*-axis and $+a$-axis pole figure has a well developed 3-fold symmetry, quartzites with such CPO occur in the Saxony granulites of amphibolite metamorphic facies near Freiberg, Germany (*e.g.* Schmid *et al.*1981, Schmid and Casey,1986).

Until now the geological view of the frequencies of finding right- or left-handed quartz crystals was based on the studies reported by Frondel (1962), where the frequency is nearly 50%:50%, which is based on measurements of large single crystals rather than polycrystalline aggregates. In chemistry it has been shown that two types of crystalline solids can be formed by chiral (enantiomorphic) crystals; a 'racemic' aggregate of 50%:50% right- and left-handed crystals, or aggregates composed uniquely of right- or left-handed forms, called homochirality created by some "symmetry breaking" process that creates an imbalance between left and right enantiomorphic crystals. The degree of imbalance is measured by Crystal Enantiomorphic Excess or CEE = (NR - NL)/(NR + NL), where NR and NL are are number of right- and left-handed crystals. Over a hundred years ago Kipping and Pope (1898) showed that seeding a crystallizing solution of sodium chlorate ($NaClO_3$ cubic space group $P2_13$, point group **23**) with right- or left-handed crystal would result in aggregate with uniquely one-hand. A number of experiments have been conducted in recent years on sodium chlorate have shown that simple action of stirring crystals floating in solution will cause homochirality (e.g. Kondepudi *et al.*,1990; Viedma,2004; Veintemillas-Verdaguer *et al.*,2007), stirred crystallization of melt (Kondepudi *et al.*,1999), crushing or grinding of crystals (Viedma,2005), boiling the solution with temperature gradient (Viedma and Cintas,2011; El Hachemi et al,2007), or shaking the solution of millimeter-sized crystals (Viedma *et al.*,2013), all processes are likely to occur in tectonic or volcanic environments of the Earth. Although the mechanism responsible for homochirality of the crystal aggregates remains controversial, the experimental results have been reproduced by several laboratories (see reviews by Weissbuch and Lahav 2011; Cintas and Viedma, 2012). Although no similar experiments have been conducted on quartz, it would be surprising that similar effects did not occur for natural crystals to explain the probable increased homochirality

in vein quartz.

Idealized symmetry models of piezoelectric properties of quartz aggregates has proposed by Zheludev (1974), and used by Parkhomenko (1971) and Bishop (1981). We develop modelling polycrystalline aggregates of Zheludev (1974) by using the ideal symmetry groups with n-fold axis, where n = ∞ is called limiting or Curie groups. There are seven limiting groups, but only three $\boldsymbol{\infty}$,$\boldsymbol{\infty mm}$ and $\boldsymbol{\infty 2}$ do not have a center of symmetry and can have piezoelectric properties (*e.g.* Zheludev, 1974). Both $\boldsymbol{\infty}$ and $\boldsymbol{\infty mm}$ have a unique polar axis can could potentially be associated with CPO of α-quartz. For example an ideal $\boldsymbol{\infty}$ right-handed quartz CPO would have the ∞-fold axis parallel to the quartz a1$[2\bar{1}\bar{1}0]$, this can implemented by `MTEX` as

```
% Default Dirichlet kernel when calculating physical properties from odf
% Band-width = Lmax = 3 for piezoelectric properties (tensor 3th rank)
% axial direction : a1 = [2-1-10] quartz
a1_direction = Miller(2,-1,-1,0,CS,'uvw','phase','Quartz')
% setup Dirichlet kernel
K_Dirichlet = kernel('Dirichlet','bandwidth',3)
% calcluate fibre odf with a1 crystal parallel x specimen
Odf_Model_A_Dirichlet = fibreODF(a1_direction,zvector,K_Dirichlet)
% RH Voigt average from odf_qtz_fourier
[d_RH_Voigt_Model_A_Quartzite_ODF_Dirichlet] = ...
    calcTensor(Odf_Model_A_Dirichlet,...
    d_RH_quartz,'Voigt')
```

```
a1_direction = Miller (show methods, plot)
  size: 1 x 1
  options: uvw
  mineral: Quartz (-3m, X||a*, Y||b, Z||c*)
  u  2
  v -1
  t -1
  w  0

K_Dirichlet = kernel (show methods, plot)
  type: Dirichlet, hw = 37

Odf_Model_A_Dirichlet = ODF (show methods, plot)
  crystal symmetry: Quartz (-3m, X||a*, Y||b, Z||c*)
  sample symmetry : triclinic

  Fibre symmetric portion:
    kernel: Dirichlet, hw = 37
    center: <2-1-10>-001
    weight: 1

d_RH_Voigt_Model_A_Quartzite_ODF_Dirichlet = tensor (show methods, plot)
  rank: 3 (3 x 3 x 3)

  tensor in compact matrix form:
```

```
       0        0        0   0.0356   0.9611        0
       0        0        0   0.9611  -0.0356        0
  0.9611   0.9611  -1.9222        0        0        0
```

From this calculation we deduce that the ∞ $d_{31} = d_{32} = d_{24} = d_{15}$ = single crystal quartz $\frac{-d_{11}}{2}$, d_{33} = single crystal quartz d_{11} and d_{14} and d_{25} = single crystal quartz $\frac{-d_{14}}{4}$ and $\frac{d_{14}}{4}$ respectively. The Figure 11 shows the maximum of -1.92 pC/N value parallel to X as expected and it value is 100% of the single crystal in the +a1$[2\bar{1}\bar{1}0]$ direction, indicating that no bias or smoothing is introduced into the ODF when using the Dirichlet kernel for physical properties. The $\boldsymbol{\infty mm}$ symmetry would require more complex microstructure in an aggregate composed of right- and left-handed crystals with ∞-fold axis parallel to the quartz a1$[2\bar{1}\bar{1}0]$ direction as before, but with two mirror planes (one normal to the symmetry axis and parallel to the symmetry axis) resulting is 4-fold disposition of the positive a1-axes in the basal plane (Zheludev, 1974), which seems unlikely in quartz. Alternatively it is more probable in tourmaline $\boldsymbol{3m}$ point group symmetry with mirror planes. The $\boldsymbol{\infty 2}$ symmetry with a two-fold axis normal to the symmetry axis has no polar axes. This symmetry of piezoelectric property could result from right-handed quartz with a CPO having the ∞-fold axis parallel to the quartz c[0001] parallel to specimen z-direction and two-fold a-axes normal to the symmetry axis, by doing a similar calculation to above, we find that the only two non-zero coefficients are d_{14} and d_{25}= single crystal quartz $\frac{d_{14}}{2}$ and $\frac{-d_{14}}{2}$ respectively. There are no polar axes because the only non-zero coefficients are two shear terms and no polarization can be generated parallel to compressive stress (longitudinal effect) can occur, and piezoelectric polarization can only be generated by applying shear stresses. The $\boldsymbol{\infty 2}$ has the same non-zero coefficients as the crystal points groups **422** and **622** for which we demonstrated that $d'_{11} = 0$.

4 Conclusions

We have extended the functions of `MTEX` to include the calculation of anisotropic crystal physical properties of 3^{rd} rank Cartesian tensors. The functions can be applied to tensors of single or polycrystalline materials. The implementation of the average tensor of polycrystalline and multi-phase aggregates using the Voigt average have been made using three routes; a) the weighted summation for individual orientation data (*e.g.* EBSD, ECPs), b) the weighted integral of the ODF, and c) using the Fourier coefficients of the ODF. Special attention has been paid to the crystallographic reference frame used for orientation data (*e.g.* Euler angles) and Cartesian tensors, as they dependent on the origin of the orientation and tensor data. Specifically piezoelectric properties the 2D and 3D representation allows a better appreciation of the often complex 3D the distribution of the different electrical polarizations and their signs. Uniform ODFs will result in a zero piezoelectric tensor for all aggregates of piezoelectric crystals, for enantiomorphic crystals aggregates composed of equal volumes of right- and left-handed crystals with the same ODF will also result in a zero piezoelectric tensor. Processes such as stirring or shaking crystals floating in solution, crushing or grinding can cause homochirality and will lead to aggregates with

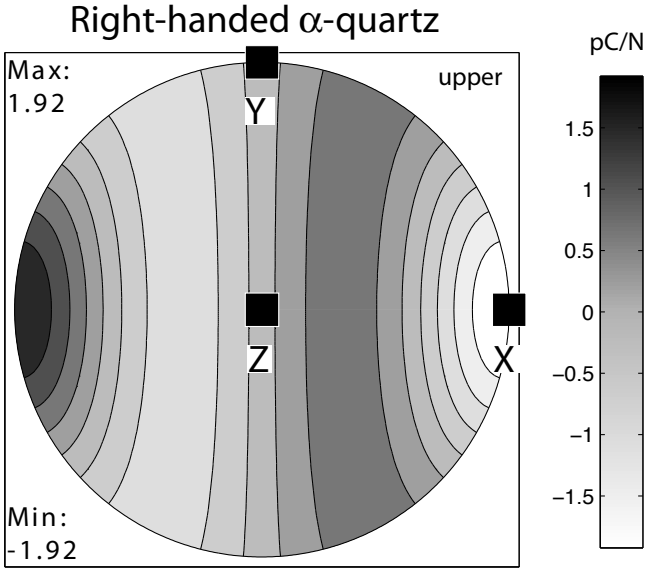

Figure 12: The pole figure of the Voigt average for piezoelectric strain tensor $\boldsymbol{d}$ for right-handed α-quartz assuming the $\boldsymbol{\infty}$ Curie group symmetry with the positive a1-axis parallel to the ∞-fold symmetry axis. The Voigt average was calculated using an ODF constructed using `fibreODF` command with Dirichlet kernel with bandwidth of three. Upper hemisphere projection. X is lineation and Z is the normal to the foliation. **N.B.** the maximum magnitude is $\pm$ 1.92 pC/N that is 100% of the single crystal.

a high piezoelectric anisotropy. When searching for ODFs that will produce aggregates with a maximum piezoelectric effect a good understanding of the single crystal properties is essential, in the case of quartz the so-called Y maximum CPO with c-axes parallel to the specimen Y-axis would appear to be a good candidate. In the case of quartz the elastic wave velocity is virtually unaffected (less than 1%) by piezoelectric coupling, in other materials the effect is very important, for wave speed anisotropy may be increased by 2 to 3 times, for example Zincite, in other examples there is almost no effect. Modelling of the effect of the *ODF* on can be simply implemented by using `fibreODF` command, either a simple verification of the Curie symmetry group for α-quartz as illustrated here, or using a combination of model *ODFs*.

The ensemble of `MTEX` functions can be used to construct project specific MatLab M-files, to process orientation data of any type in a coherent work-flow from the texture analysis to the anisotropic physical properties. A wide range of graphical tools provides publication quality output in a number of formats. The construction of M-files for specific problems provides a problem-solving method for teaching elementary to advanced texture analysis and anisotropic physical properties. The open source nature of this project (http://mtex.googlecode.com) allows researchers to access all the details of their calculations, check intermediate results and further the project by adding new functions on Linux, Mac OS X or Windows platforms.

Acknowledgments

It is pleasure for DM to dedicate this paper to Prof. Ernie Rutter who introduced him to the representation of physical properties of crystals by tensors, and many other things, as part of his Masters course at Imperial College, London.

The authors gratefully acknowledge that this contribution results form scientific cooperation on the research project "Texture and Physical Properties of Rocks", which has been funded by the French-German program EGIDE-PROCOPE. This bilateral program is sponsored by the German Academic Exchange Service (DAAD) with financial funds from the federal ministry of education and research (BMBF) and the French ministry of foreign affairs.

The authors thank the two reviewers for the hard work involved in reviewing such a technical manuscript, their checking of some of the equations eliminated some typing errors and helpful comments improved our paper.

References

[1] ANSI-IEEE 176, 1987. Standard on Piezoelectricity. DOI: 10.1109/IEEESTD.1988.79638

[2] Auld, B.A., 1990. Acoustic Fields and Waves in Solids (Two Volumes). Malabar, Florida: Krieger Publishing Co.

[3] Bachmann, F., Hielscher, H., Jupp, P. E., Pantleon, W., Schaeben, H. & Wegert, E.: 2010. Inferential statistics of electron backscatter diffraction data from within individual crystalline grains. J. Appl. Cryst. 43, 1338-1355

[4] Bazhenov,A.V. 1961. Piezoelectric Properties of Wood. Consultants Bureau. New York, N.Y.

[5] Bechmann, R., 1958. Elastic and piezoelectric constants of alpha-quartz. Physical Review, 110, 1060-1061.

[6] Bishop, J.R., 1981. Estimating quartz fabrics from piezoelectric measurements. Math. Geol., 13, 261 - 289.

[7] Bishop, J.R. and Emerson, D.W., 1999. Geophysical properties of zinc-bearing deposits. Australian Journal of Earth Sciences, 46, 311-328.

[8] Bond, W.L., 1943. The mathematics of the physical properties of crystals. Bell Syst. Tech. J. XXII, 1-72.

[9] Brainerd, J.G., et al.,1949. Standards on piezoelectric crystals, Proc. Inst. Radio Eng. 37,1378-1395.

[10] Bunge, H.J., 1969, Mathematische methoden der texturanalyse, Akademie-Verlag, Berlin.

[11] Bunge, H.J. & Esling, C. 1985. Symmetries in texture analysis. Acta Cryst. A41, 59-67.

[12] Cady, W.G. 1964. Piezoelectricity. Dover Publications Inc. ,New York.

[13] Cintas, P., Viedma, C., 2012. On the Physical Basis of Asymmetry and Homochirality. Chirality, 24, 894 - 908.

[14] Cook, R.K., Weissler,P.G., 1950. Piezoelectric Constants of Alpha- and Beta-Quartz at Various Temperatures. Physical Review 80,712-716.

[15] Corry, C.E. 1994, Investigation of ferroelectric effects in two sulfide deposits, Journal of Applied Geophysics,32, 55-72.

[16] Curie,J. and Curie,P., 1880. D*é*veloppement par compression de l' *é*lectricit*é* polaire dans les cristaux h*é*mi*è*dres *à* faces inclin*é*es. Bulletin de la soci*é*t*é* min*é*ralogique de France, 3, 90-93.

[17] Curie J. and Curie,P. 1881. Contractions et dilatations produites par des tensions *é*lectriques dans les cristaux h*é*mi*è*dres *à* faces inclin*é*es. Comptes Rendus (France) 93,1137-1140.

[18] Curie,J. and Curie,P., 1882. Phénomènes électriques des cristaux hémièdres à faces inclinées, Journal de Physique théorique et appliquée, 1, 245-251.

[19] Dieulesaint, E., Royer, D. 1996 Ondes élastiques dans les solides. Tome 1, Propagation libre et guidée. Masson, Paris.

[20] Donnay, J. D. H. and Le Page, Y., 1975. Twin laws versus electrical and optical characters in low quartz. Canadian Mineralogist, 13, 83-85.

[21] Donnay, J. D. H. and Le Page, Y. 1978. The vicissitudes of the low quartz setting or the pitfalls of enantiomorphism. Acta Cryst. A34, 584 - 594.

[22] Frondel, C. 1962. The system of Mineralogy. 7th edition volume 3, Silica Minerals. John Wiley, New York.

[23] Fukada, E. and Yasuda, I., 1957. On the piezoelectric effect of bone. Journal of the physical society of Japan, 12, 1158-1162.

[24] Fukada, E. and Yasuda, I., 1964. Piezoelectric effects in collagen. Jap. J. Appl. Phys. 3, 117-121.

[25] Ganster, J., and Geiss, D. 1985. Polycrystalline simple average of mechanical properties in the general (triclinic) case. Phys. stat. sol. (b) , 132, 395-407.

[26] Ghomshei, M.M., Narod, B.B., Templeton, T.L., Arrott, A.S. and Russell, R.D., 1988. Piezoelectric pole figure of a vein quartz sample. Textures Microstructures, 7, 303 - 316.

[27] Goodman, P. & Johnston, A. W. S. 1977. Identification of enantiomorphously related space groups by electron diffraction - a second method. Acta Cryst. A33, 997-1001.

[28] Goodman, P. & Secomb, T. W. 1977. Identification of enantiomorphously related space groups by electron diffraction. Acta Cryst. A33,126-133.

[29] Hayakawra, R. & Wada, Y., 1973. Piezoelectricity and related properties of polymer films. Advan. Polymer Sci. 11, 1-55.

[30] Hielscher, R., & Schaeben, H., 2008, A novel pole figure inversion method: specification of the MTEX algorithm. Journal of Applied Crystallography, 41 ,1024-1037.doi:10.1107/S0021889808030112

[31] Haussühl, S. ,1991 Pyroelectric, dielectric, piezoelectric, elastic and thermoelastic properties of triclinic lithium hydrogen Oxalate monohydrate, $LiHC_20_4.H_20$. Zeitschrift für Kristallographie, 194, 57-65.

[32] Heckmann, G.,1925 Die Gittertheorie der festen Köper. Ergeb Exakten Naturwiss 4, 100-153.

[33] Hermann, C.,1934. Tensoren und Kristallsymmetrie. Z. Kristallogr. 89, 32-48.

[34] Hielscher,R., 2010. Kernel density estimation on the rotation group, Preprint, Fakultät für Mathematik, TU Chemnitz.

[35] Hielscher, R., Schaeben, H. Siemes, H., 2010. Orientation distribution within a single hematite crystal. Math. Geosci., 42, 359-375.

[36] Hielscher, R., & Schaeben, H., 2008, A novel pole figure inversion method: specification of the MTEX algorithm. Journal of Applied Crystallography, 41 ,1024-1037.doi:10.1107/S0021889808030112

[37] Ikeda, T., 1990. Fundamentals of Piezoelectricity. Oxford University Press.

[38] Jaffe B., Cook W.R., Jaffe H., 1971. Piezoelectric Ceramics. Academic Press, New York.

[39] Jung, I.H., and Auh,K.H., 1999. Crystal growth and piezoelectric properties of langasite ($La_3Ga_5SiO_{14}$) crystals. Materials Letters 41, 241-246.

[40] Kerkoc,P., Maruo,S., Horinouchi,S. and Sasaki,K.,1990. Piezoelectric and electro-optic coefficients of the molecular nonlinear optical crystal 2-furyl methacrylic anhydride. Applied physics Letters, 74,3105 - 3106.

[41] Kipping, W.S., Pope W.J. 1898. Enantiomorphism. J Chem Soc Trans 73, 606-617.

[42] Klapper, H. and Hahn, Th., 2006. Point-group symmetry and physical properties of crystals, in International Tables for Crystallography 2006. Vol. A, Chapter 10.2, 804-808. Dordrecht: Kluwer Academic Publishers.

[43] Kobiakov, I. B. 1980. Elastic, Piezoelectric and dielectric properties of ZnO and CdS single crystals in a wide range of temperatures. Sol. St. Comm., 35, 305-310.

[44] Kondepudi,D.K., Kaufmann, R. and Singh, N. 1999.Chiral Symmetry Breaking in Sodium Chlorate Crystallization. Science 250, 975 - 976.

[45] Kondepudi,D.K., Laudadio,J. and Asakura,K. 1999. Chiral Symmetry Breaking in Stirred Crystallization of 1,1'-Binaphthyl Melt. J. Am. Chem. Soc. 121, 1448-1451.

[46] Lloyd, G.E., Ferguson, C.C., Law, R.D. 1987. Discriminatory petrofabric analysis of quartz rocks using SEM electron channelling. Tectonophysics 135, 243-249.

[47] Le Page, Y., Saxe, P., Rodgers, J.R. 2002. *Ab initio* stiffness for low quartz and calcite. phys. stat. sol. (b),229, 1155 - 1161.

[48] Li, J.Y and Dunn, M.L., 2001.Variational bounds for the effective moduli of heterogeneous piezoelectric solids.Philosophical Magazine A, 81, 903 - 926.

[49] Lippmann, G. 1881. Principe de la conservation de l'*é*lectricit*é*. Annales de chimie et de physique. 24, 145-177.

[50] Mainprice, D., Lloyd, G.E. and Casey, M. 1993. Individual orientation measurements in quartz polycrystals - advantages and limitations for texture and petrophysical property determinations. J.Struc.Geol. 15, 1169-1187.

[51] Mainprice, D. & Humbert, M., 1994. Methods of calculating petrophysical properties from lattice preferred orientation data. Surveys in Geophysics 15, 575-592.

[52] Mainprice, D., Hielscher,R., & Schaeben,H., 2011, Calculating anisotropic physical properties from texture data using the MTEX open-source package. Prior, D. J., Rutter, E. H. & Tatham, D. J. (eds) Deformation Mechanisms, Rheology and Tectonics: Microstructures, Mechanics and Anisotropy. Geological Society, London, Special Publications, 360, 175-192. DOI: 10.1144/SP360.10

[53] Marthinsen, K. & Høier, R. 1988. On the breakdown of Friedel's law in electron backscattering. Acta Cryst. A44, 700-707.

[54] Mason, W.P., 1966. Crystal Physics of Interaction Processes. Academic Press, New York.

[55] Messing, G. L., Trolier-McKinstry, S., Sabolsky, E. M., Duran, C., Kwon, S., Brahmaroutu, B., Park, P., Yilmaz, H., Rehrig, P. W., Eitel, K. B., Suvaci, E., Seabaugh, M. and Oh, K. S. 2004. 'Templated Grain Growth of Textured Piezoelectric Ceramics', Critical Reviews in Solid State and Materials Sciences, 29, 45 - 96.

[56] Morris, P.R., 2006. Polycrystalline elastic constants for triclinic crystal and physical symmetry, J. Applied Crystal., 39,502-508.

[57] Neishtadt, N.M., Eppelbaum, L.V., Levitski, A.G. 2006. Application of piezoelectric and seismoelectrokinetic phenomena in exploration geophysics: Review of Russian and Israeli experiences.Geophysics, 71, B41-B53. 10.1190/1.2187714

[58] Newnham, R.E., 2005. Properties of materials Anisotropy, Symmetry, Structure.Oxford University Press,Oxford.

[59] Nye, J. F., 1985. Physical Properties of Crystals: Their Representation by Tensors and Matrices, 2nd ed., Oxford Univ. Press, England.

[60] Ogi,H., Fukunaga,M., and Masahiko Hirao,M.,2004 Elastic constants, internal friction, and piezoelectric coefficient of $\alpha - TeO_2$. Phys. Rev. B 69, 024104.

[61] Ogi, H., Ohmori, T. Nakamura, N. and Hirao M., 2006. Elastic, anelastic and piezoelectric coefficients of alpha-quartz determined by resonance ultrasound spectroscopy. Journal of Applied Physics, 100, 053511.

[62] Reuss, A., 1929. Berechnung der Fließrenze von Mischkristallen auf Grund der Plastizitätsbedingung für Einkristalle, Z. Angew. Math. Mech. 9, 49-58.

[63] Russell,R.D., Ghomshei,M.M., 1997. Inverting piezoelectric measurements. Tectonophysics, 271, 21-35.

[64] Schmid, S.M., Casey, M., 1986. Complete fabric analysis of some commonly observed quartz c-axis patterns. In: Heard, H.C., Hobbs, B.E. (Eds.), Mineral and Rock Deformation: Laboratory Studies, The Paterson Volume, Series, vol. 36, AGU monograph, Washington, pp. 263-286.

[65] Schmid, S.M., Casey, M., Starkey, J., 1981. An illustration of the advantage of a complete texture analysis described by the orientation distribution function (ODF) using quartz pole figure data. Tectonophysics 78, 101-117.

[66] Sirotin, Yu.I. & Shakolskaya, M.P., 1982. Fundamentals of Crystal Physics. Mir, Moscow. pp 654.

[67] Taylor, S. R. & McLennan, S. M. (1985). The Continental Crust: Its Composition and Evolution. Blackwell (Oxford), 312pp.

[68] Tichý,J., Erhart, J., Kittinger, E. & P*ř́*ivratská, J.,2010. Fundamentals of Piezoelectric Sensorics, Springer-Verlag, Berlin,pp 207.

[69] Veintemillas-Verdaguer, S., Osuna Esteban,S., Herrero,M.A., 2007 The effect of stirring on sodium chlorate crystallization under symmetry breaking conditions; Journal of Crystal Growth 303, 562 - 567.

[70] Viedma, C., 2004. Experimental evidence of chiral symmetry breaking in crystallization from primary nucleation. Journal of Crystal Growth 261, 118 -121.

[71] Viedma, C., 2005. Chiral symmetry breaking during crystallization: Complete chiral purity induced by nonlinear autocatalysis and recycling. Phys Rev Lett 94: 065504.

[72] Viedma, C., Cintas, P., 2011. Homochirality beyond grinding: deracemizing chiral crystals by temperature gradient under boiling. Chem Commun, 47, 12786 - 12788.

[73] Viedma,C., McBride, J.M., Kahr,B., and Pedro Cintas, P. 2013 Enantiomer-Specific Oriented Attachment: Formation of Macroscopic Homochiral Crystal Aggregates from a Racemic System. Angew. Chem. Int. Ed. 52, 10545 - 10548.

[74] Voigt,W., 1898. Die fundamentalen physiklischen Eigenschaften der Kristalle,Teubner-Verlag,Leipzig.

[75] Voigt,W., 1887. Gessellschaft der wussebschaften ub Gottingen, 34 ,3-52.

[76] Voigt,W., 1910. Lehrbuch der Kristallphysik, Teubner-Verlag,Leipzig.

[77] Voigt,W., 1928. Lehrbuch der Kristallphysik, Teubner-Verlag,Leipzig.

[78] Wan Y P, Xie L T, Zhong Z., 2012. Variational bounds of the effective moduli of piezoelectric composites. Sci China-Phys Mech Astron, 55, 2106-2113, doi: 10.1007/s11433-012-4706-9

[79] Warner,A. W., Onoe,M., Coquin,G. A. 1967. Determination of Elastic and Piezoelectric Constants for Crystals in Class (3m). J. Acoust. Soc. Am. Volume 42, 1223-1231.

[80] Weissbuch,I. and Lahav,M., 2011 Crystalline Architectures as Templates of Relevance to the Origins of Homochirality. Chem. Rev. 2011, 111, 3236 - 3267. dx.doi.org/10.1021/cr1002479

[81] Wenk, H.-R. 1985. Measurement of pole figures in 'Preferred Orientation in Metals and Rocks: An Introduction to Modern Textural Analysis' Edited by Wenk, H.-R., Academic Press,Orlando.

[82] Zheludev, I.S.,1974. Piezoelectricity in textured media. Solid State Physics 29, 315-360.

Tensor	Rank	Symbol	S.I. Units
Elastic strain	2^{nd}	ε_{ij}	dimensionless
Elastic stress	2^{nd}	σ_{ij}	Pa
Electric field	1^{st}	E_i	V m^{-1}
Electric displacement	1^{st}	D_i	C m^{-2}
Dielectric permittivity	2^{nd}	κ_{ij}	F m^{-1}
Dielectric impermeability	2^{nd}	β_{ij}	m F^{-1}
Dielectric polarization	1^{st}	P_i	C m^{-2}
Elastic stiffness	4^{th}	c_{ijkl}	Pa
Elastic compliance	4^{th}	s_{ijkl}	Pa^{-1}
Piezoelectric strain	3^{rd}	d_{ijk}	C N^{-1} *or* m V^{-1}
Piezoelectric strain	3^{rd}	g_{ijk}	V m N^{-1} *or* m^2 C^{-1}
Piezoelectric stress	3^{rd}	e_{ijk}	C m^{-2} *or* N $V^{-1}m^{-1}$
Piezoelectric stress	3^{rd}	h_{ijk}	V m^{-1} *or* N C^{-1}

Table 1: Symbols and units used for tensors this paper. When a symbol is used as superscript means constant value of D, E, ε or σ during measurement. Units may also be pico (10^{-12}) *e.g.* pC, or giga (10^9) *e.g.* GPa

Property	IRE 1949 RH-Quartz	IRE 1949 LH-Quartz	IEEE 1978 RH-Quartz	IEEE 1978 LH-Quartz
Elastic Compliance tensor s_{14}	+	+	-	-
Elastic Stiffness tensor c_{14}	-	-	+	+
Piezoelectric strain tensor d_{11}	-	+	+	-
Piezoelectric strain tensor d_{14}	-	+	-	+
Piezoelectric stress tensor e_{11}	-	+	+	-
Piezoelectric stress tensor e_{14}	+	-	+	-

Table 2: Conventions for the signs of constants in right- and left-handed α-quartz (simplfied after Tichý et al.,2010)
N.B. all constants measured in a right-handed Cartesian coordinate system
LePage et al.(2002) right-handed α-quartz c_{14} = - 19.7 GPa

Right-handed α-quartz

c_{ij}^E GPa	d_{ij} 10^{-12} CN^{-1}	g_{ij} m^{2}C^{-1}	e_{ij} Cm^{-2}	h_{ij} 10^9NC^{-1}	κ_{ij}^σ 10^{-12}mf^{-1}
c_{11}^E= 86.76	d_{11}=-1.9222	g_{11}=-0.0481	e_{11}=-0.1510	h_{11} =-3.8512	κ_{11}^σ = 39.17
c_{12}^E= 6.868	d_{14}=-0.1423	g_{14}=-0.0036	e_{14}=+0.0610	h_{14} =+1.5558	κ_{33}^σ = 41.01
c_{13}^E= 11.85					
c_{14}^E= -18.02					
c_{33}^E= 105.46					
c_{44}^E= 58.14					

Left-handed α-quartz

c_{ij}^E GPa	d_{ij} 10^{-12} CN^{-1}	g_{ij} m^{2}C^{-1}	e_{ij} Cm^{-2}	h_{ij} 10^9NC^{-1}	κ_{ij}^σ 10^{-12}mf^{-1}
c_{11}^E= 86.76	d_{11}=+1.9222	g_{11}=+0.0481	e_{11}=+0.1510	h_{11} =+3.9820	κ_{11}^σ = 39.17
c_{12}^E= 6.868	d_{14}=+0.1423	g_{14}=+0.0036	e_{14}=-0.0610	h_{14} =-1.9778	κ_{33}^σ = 41.01
c_{13}^E= 11.85					
c_{14}^E= -18.02					
c_{33}^E= 105.46					
c_{44}^E= 58.14					

Table 3: Properties of α-quartz according to IRE 1949 standard. Original data on e_{ij}, c_{ij}^E and κ_{ij}^σ from Ogi, H., Ohmori, T. Nakamura, N. and Hirao M. (2006) Journal of Applied Physics, 100, 053511. Only the independent non-zero tensor coefficients are listed. c_{ij}^E = Adiabatic elastic stiffness tensor at constant electric field d_{ij} and g_{ij} = Piezoelectric strain tensors e_{ij} and h_{ij} = Piezoelectric stress tensors κ_{ij}^σ = Dielectric permittivity tensor at constant stress.